scientific reports

Check for updates

OPEN

Computational analysis of antimicrobial peptides targeting key receptors in infection-related cardiovascular diseases: molecular docking and dynamics insights

Doni Dermawan[1] & Nasser Alotaiq[2]✉

Infection-related cardiovascular diseases (CVDs) pose a significant health challenge, driving the need for novel therapeutic strategies to target key receptors involved in inflammation and infection. Antimicrobial peptides (AMPs) show the potential to disrupt pathogenic processes and offer a promising approach to CVD treatment. This study investigates the binding potential of selected AMPs with critical receptors implicated in CVDs, aiming to explore their therapeutic potential. A comprehensive computational approach was employed to assess AMP interactions with CVD-related receptors, including ACE2, CRP, MMP9, NLRP3, and TLR4. Molecular docking studies identified AMPs with high binding affinities to these targets, notably Tachystatin, Pleurocidin, and Subtilisin A, which showed strong interactions with ACE2, CRP, and MMP9. Following docking, 100 ns molecular dynamics (MD) simulations confirmed the stability of AMP-receptor complexes, and MM/PBSA calculations provided quantitative insights into binding energies, underscoring the potential of these AMPs to modulate receptor activity in infection and inflammation contexts. The study highlights the therapeutic potential of Tachystatin, Pleurocidin, and Subtilisin A in targeting infection-related pathways in CVDs. These AMPs demonstrate promising receptor binding properties and stability in computational models. Future research should focus on in vitro and in vivo studies to confirm their efficacy and safety, paving the way for potential clinical applications in managing infection-related cardiovascular conditions.

Keywords Antimicrobial peptides, Cardiovascular disease, Molecular Docking, Molecular dynamics

Abbreviations

ACE2	Angiotensin-converting enzyme 2
AMPs	Antimicrobial peptides
CRP	C-reactive protein
CVDs	Cardiovascular diseases
GRAVY	Grand average of hydropathicity
HAPPENN	Hemolytic activity prediction for peptides and proteins
IC	Intermolecular contact
MD	Molecular dynamics
MDR	Multidrug-resistant
MM/PBSA	Molecular Mechanics/Poisson–Boltzmann Surface Area
MMPs	Matrix metalloproteinases
NIS	Non-interacting surface
OPLS-AA/L	Optimized potentials for liquid simulations
PAMPs	Pathogen-associated molecular patterns
RMSD	Root mean square deviation
RMSF	Root mean square fluctuation

[1]Applied Biotechnology, Faculty of Chemistry, Warsaw University of Technology, Warsaw 00-661, Poland. [2]Health Sciences Research Center (HSRC), Imam Mohammad Ibn Saud Islamic University (IMSIU), Riyadh 13317, Saudi Arabia. ✉email: naalotaiq@imamu.edu.sa

RoG	Radius of gyration
SCOP	Structural classification of proteins
SPCE	Single point charge extended
TLRs	Toll-like receptors

Background

Infections and cardiovascular diseases (CVDs) share a complex, bidirectional relationship. Infections can serve as both a cause and a consequence of CVDs, with significant implications for disease progression and patient outcomes[1]. Pathogenic microorganisms can directly infect cardiovascular tissues, exacerbate existing conditions, or initiate cardiovascular events through systemic inflammatory responses and immune system dysregulation. Conversely, cardiovascular conditions such as heart failure and ischemic events can increase susceptibility to infections due to impaired immunity and compromised organ function[2,3]. Pathogenic microorganisms can initiate or exacerbate CVDs through direct infection of cardiovascular tissues, immune system dysregulation, or the induction of chronic inflammatory states[4,5]. For instance, respiratory pathogens such as influenza virus and bacterial pathogens like *Chlamydia pneumoniae* and *Helicobacter pylori*have been associated with an increased risk of myocardial infarction and atherosclerosis[6,7]. The chronic inflammation induced by these pathogens accelerates the formation of atherosclerotic plaques, a major cause of coronary artery disease. Among the most prominent mechanisms is the activation of the innate immune system via receptors such as Toll-Like Receptors (TLRs), which recognize pathogen-associated molecular patterns (PAMPs)[8–10]. TLRs initiate signaling cascades upon activation that produce pro-inflammatory cytokines, resulting in endothelial dysfunction and plaque instability. Another key player in this inflammatory process is the NLRP3 inflammasome, which responds to infectious and non-infectious stimuli, including viral RNA, bacterial toxins, and cholesterol crystals[11,12]. Once activated, the NLRP3 inflammasome promotes the secretion of IL-1β, a potent pro-inflammatory cytokine implicated in the progression of atherosclerosis[13,14]. Furthermore, angiotensin-converting enzyme 2 (ACE2), a receptor known for regulating blood pressure, has gained considerable attention due to its interaction with the SARS-CoV-2 virus[15,16]. The binding of the virus to ACE2 receptors impairs its physiological functions, leading to cardiovascular complications, including myocardial injury and arrhythmias[17]. Matrix metalloproteinases (MMPs), a family of proteolytic enzymes involved in extracellular matrix remodeling, also play a critical role in CVD progression, particularly in the degradation of the fibrous cap of atherosclerotic plaques, leading to plaque rupture and subsequent cardiovascular events[18,19]. While MMP9 is primarily recognized as a target enzyme, it may also exhibit receptor-like characteristics through its interactions with various signaling molecules, highlighting its dual role in inflammation and cardiovascular pathology. Together, these pathways highlight the multifaceted interactions between infections and CVDs, underscoring the need for integrated therapeutic approaches.

Treating infections related to cardiovascular diseases typically involves using antimicrobial agents such as antibiotics, antivirals, and antifungals, depending on the pathogen involved. For bacterial infections, antibiotics such as macrolides and β-lactams are commonly prescribed. For example, azithromycin is often used to treat *Chlamydia pneumoniae*infections associated with atherosclerosis[20,21]. However, the use of antibiotics poses several challenges, including the emergence of antibiotic resistance, which has become a significant global health threat. The overuse and misuse of antibiotics have led to the development of multidrug-resistant (MDR) strains, which are not only harder to treat but also contribute to higher mortality rates in patients with CVDs[22–24]. Moreover, the long-term use of antibiotics has been associated with adverse cardiovascular outcomes, including arrhythmias and QT interval prolongation[25]. As a result, there is growing interest in exploring alternative therapeutic strategies, such as the use of antimicrobial peptides (AMPs), which have the potential to overcome the limitations of current therapies and provide more targeted interventions. One of the significant advantages of AMPs is their ability to selectively target microbial membranes, which reduces the likelihood of developing resistance compared to traditional antibiotics[26,27]. Unlike conventional antimicrobial agents that often target specific bacterial proteins or enzymes, AMPs disrupt microbial membranes by interacting with their lipid bilayers, leading to cell lysis and death[28]. This mode of action is less prone to resistance, as microbes would need to undergo significant changes in membrane composition to evade AMP activity[29,30].

In silico methods, including molecular docking and molecular dynamics (MD) simulations, offer significant advantages in understanding the interactions between proteins and potential therapeutic compounds[31,32]. These computational techniques enable detailed insights into the molecular mechanisms underlying diseases, including those related to infection-induced cardiovascular conditions. For instance, MD simulations can provide a deeper understanding of how mutations impact protein function and lead to pathological outcomes, facilitating the identification of new therapeutic targets[33]. Similarly, in silico approaches are instrumental in drug discovery, enabling the design of novel compounds by evaluating their binding affinity, stability, and potential side effects before experimental validation[34,35]. Additionally, MD simulations can optimize the solubility and therapeutic potential of bioactive compounds by simulating interactions with carrier molecules[36]. These methodologies are powerful tools for enhancing the design of effective, selective, and safer therapeutic agents, which is crucial for exploring innovative strategies to combat infection-related cardiovascular diseases using AMPs.

The rationale of this study lies in the need to explore alternative therapeutic strategies that address the limitations of current treatments for infection-related CVDs. AMPs have garnered significant attention for their broad-spectrum antimicrobial properties, reduced propensity for resistance development, and immunomodulatory effects. AMPs, small naturally occurring molecules, disrupt microbial membranes and reduce inflammation, distinguishing them from traditional antimicrobial agents. Furthermore, their potential to interact with critical CVD-related receptors, such as TLRs, ACE2, and NLRP3, suggests a role in modulating microbial infections and the associated inflammatory pathways that drive CVD progression. This study aimed

to explore the potential of AMPs to bind with key receptors involved in infection-related CVDs, offering insights into their role in modulating receptor interactions. By employing a comprehensive in silico approach, including molecular docking and molecular dynamics simulations, we assessed the interaction dynamics, stability, and binding affinities of various AMPs with critical CVD-related receptors. This study aims to provide insights into the potential role of AMPs in modulating receptor interactions, which may pave the way for the development of novel peptide-based therapies targeting infection-driven cardiovascular and inflammatory conditions.

Results

Molecular docking simulations of AMPs and receptors implicated in infection-related CVDs

The best binding poses of AMPs and ACE2 (as one of the target receptors) are presented in Fig. 1. The HADDOCK score provided an overall measure of the docking quality by integrating both the spatial and energetic fit of the AMP to the receptor. Free binding energy, measured in kilocalories per mole, offered a quantitative assessment of the binding strength between the AMPs and the receptors[37]. The van der Waals and electrostatic energies were also analyzed to gain insight into the non-covalent forces driving the interactions, which are crucial for understanding how these peptides interact at the molecular level. Additionally, desolvation energy, which reflects the energy of displacing water molecules from the receptor surface upon peptide binding, was calculated to understand the binding thermodynamics[38]. These results laid the groundwork for further molecular dynamics simulations to explore the stability and dynamics of the AMP-receptor complexes.

Figure 2 presents the free binding energy (kcal/mol) scores for the top-performing AMPs interacting with different target proteins, focusing on Tachystatin, Thermolysin, Pleurocidin, and Subtilisin A as consistent performers. Tachystatin demonstrated significant binding affinity across multiple targets. When docked with ACE2, Tachystatin achieved a HADDOCK score of -102.0 ± 3.7 a.u. and a binding energy of -10.7 kcal/mol, outperforming the standard inhibitor DX600 (-8.6 kcal/mol). The van der Waals energy was -48.4 ± 4.4 kcal/mol, and the electrostatic energy was -220.9 ± 32.4 kcal/mol, reflecting strong interaction forces, while the RMSD value of 1.5 ± 0.0 Å indicates a relatively stable conformation. Tachystatin similarly showed strong binding with MMP9, achieving a HADDOCK score of -136.4 ± 3.4 a.u. and a binding energy of -12.2 kcal/mol. These results highlight Tachystatin's consistent performance across different proteins. This interaction was considered strong based on comparative analysis with the standard inhibitor results, which provided a benchmark for evaluating the binding affinity and binding energy of the AMPs.

Thermolysin was also identified as a highly effective AMP, particularly with ACE2 and NLRP3. In the ACE2 complex, Thermolysin achieved a HADDOCK score of -91.4 ± 2.4 a.u. and a binding energy of -10.7 kcal/mol, comparable to Tachystatin. Its van der Waals energy of -49.2 ± 2.5 kcal/mol and electrostatic energy of -131.8 ± 20.5 kcal/mol indicate a well-balanced interaction. Thermolysin's performance with MMP9 also stood out, yielding a binding energy of -10.6 kcal/mol with a HADDOCK score of -114.4 ± 3.8 a.u., and it demonstrated a stable RMSD of 1.2 ± 0.2 Å. Pleurocidin, another top-performing peptide, demonstrated robust binding across multiple proteins. In complex with ACE2, Pleurocidin achieved a HADDOCK score of -104.8 ± 1.9 a.u. and a

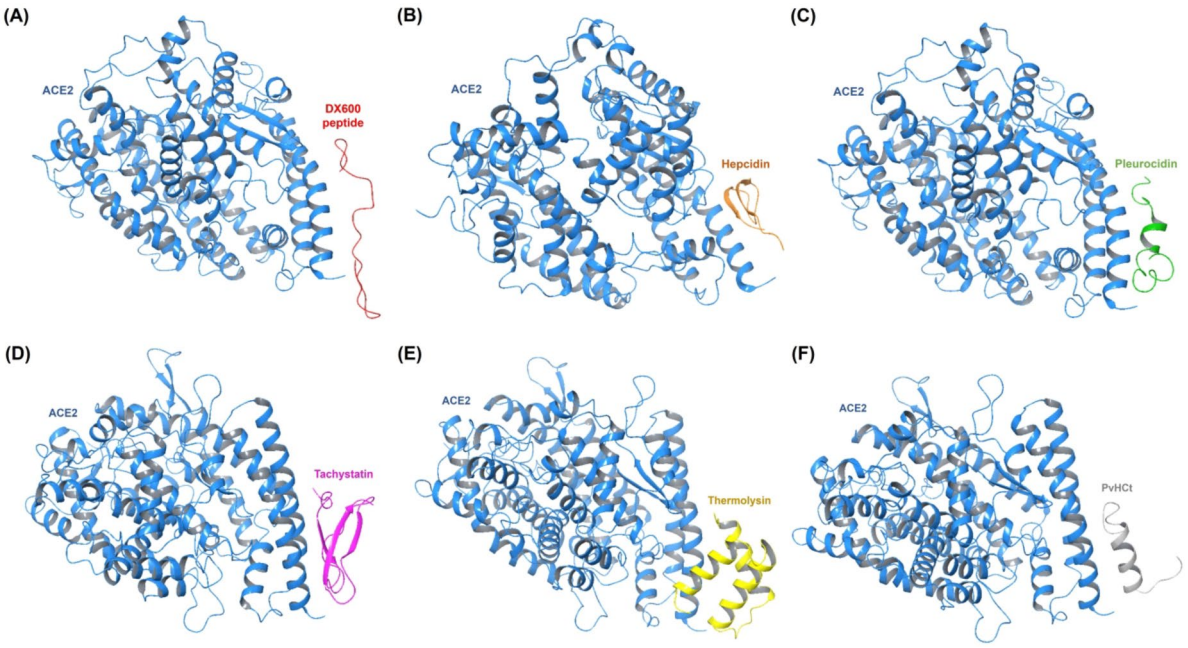

Fig. 1. Molecular docking simulations illustrate the optimal binding orientations for interactions between AMPs and ACE2. (**a**) ACE2:DX600 peptide (standard antagonist) complex. (**b**) ACE2:Hepcidin complex. (**c**) ACE2:Pleurocidin complex. (**d**) ACE2:Tachystatin complex. (**e**) ACE2:Thermolysin complex. (**f**) ACE2:PvHCt complex. The AMPs depicted were chosen based on their consistently high binding affinities from a broader set of 30 AMPs analyzed in this study.

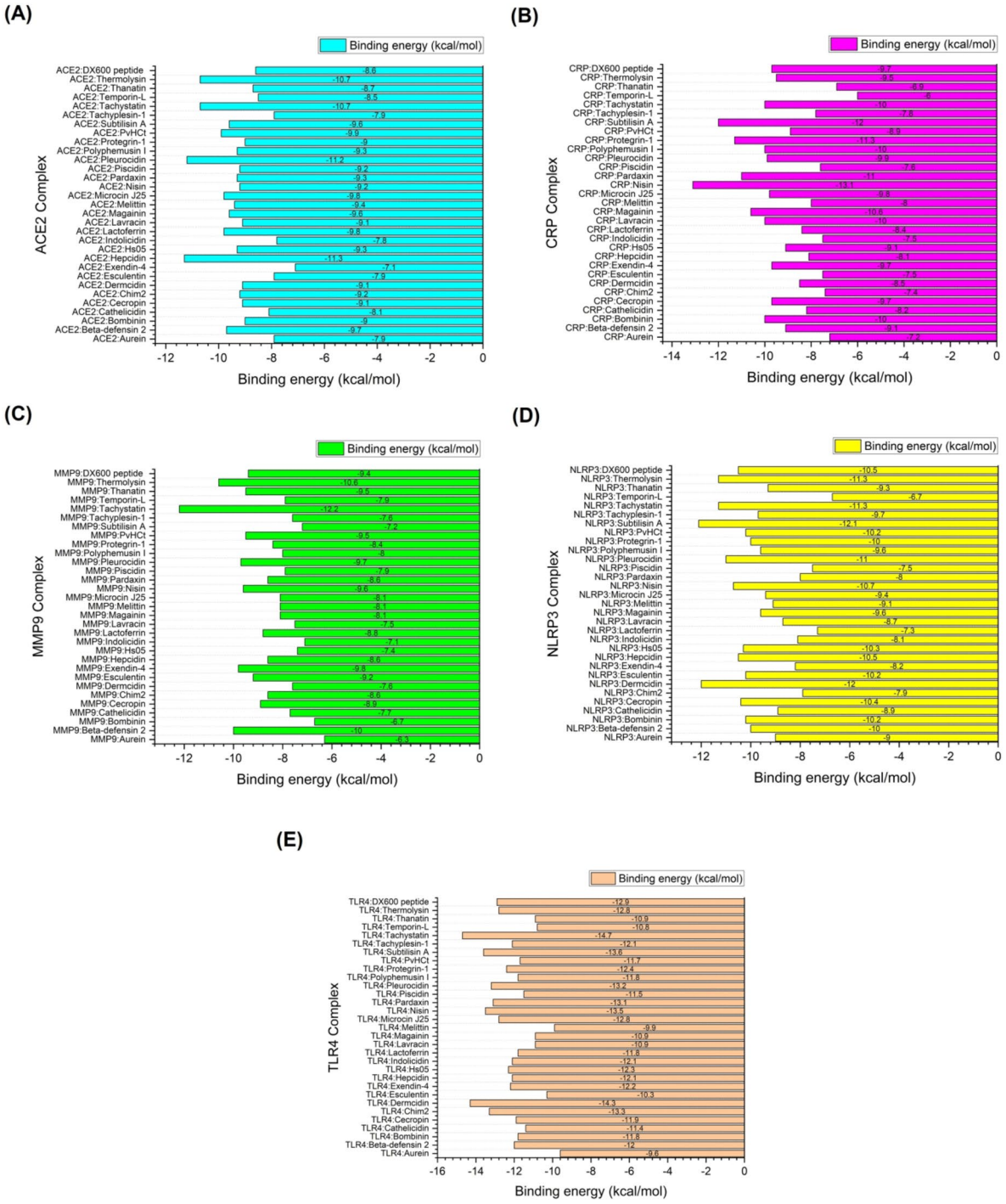

Fig. 2. Molecular docking results of optimal target receptor-AMP complexes, highlighting the lowest binding energy values indicative of a superior affinity. (**A**) ACE2 complexes. (**B**) CRP complexes. (**C**) MMP9 complexes. (**D**) NLRP3 complexes. (**E**) TLR4 complexes.

binding energy of −11.2 kcal/mol, with a van der Waals energy of −46.6 ± 6.0 kcal/mol and an electrostatic energy of −220.6 ± 23.5 kcal/mol, indicating strong non-covalent interactions. Similarly, Pleurocidin exhibited a strong interaction with MMP9, with a HADDOCK score of −143.7 ± 4.0 a.u. and a binding energy of −9.7 kcal/mol. The stability of these interactions was underscored by an RMSD of 1.2 ± 0.1 Å. Subtilisin A demonstrated strong binding interactions, particularly with CRP and NLRP3. In the CRP complex, Subtilisin A achieved a HADDOCK score of −128.1 ± 8.3 a.u. and a binding energy of −12.0 kcal/mol, significantly surpassing the binding energy of DX600 (−9.7 kcal/mol). The electrostatic energy was − 306.9 ± 57.8 kcal/mol, indicating powerful electrostatic interactions, while the RMSD value of 0.6 ± 0.5 Å reflects a stable interaction. In the NLRP3 complex, Subtilisin

A showed similar effectiveness, with a HADDOCK score of −138.7 ± 2.8 a.u. and a binding energy of −12.1 kcal/mol, demonstrating its strong and consistent performance. The results, as summarized in Table 1, demonstrate the strong binding affinity and stability of the top-performing AMPs—particularly Tachystatin, Thermolysin, Pleurocidin, and Subtilisin A—toward key protein targets implicated in infection pathways related to CVDs. These AMPs exhibit the potential to inhibit receptor-mediated adhesion and signaling processes, which play a critical role in infection onset and progression. Their stable interactions with these receptors suggest promising therapeutic applications in preventing CVD-associated infections. Detailed molecular docking results are available in Supplementary Data 1.

The correlation matrix further emphasizes the structural implications of these findings, revealing that specific receptor residue interactions are strongly correlated with the binding energies of the AMPs. This correlation suggests that the binding affinity of AMPs is not solely dependent on the overall molecular shape but also on the interactions at critical residue sites within the receptor-binding pockets. For instance, the key residues identified in Tachystatin and Pleurocidin, such as specific charged or hydrophobic residues, play a pivotal role in stabilizing the AMP-receptor complex. By focusing on optimizing interactions with these residues, it may be possible to design AMPs with enhanced specificity and strength of binding. The matrix also highlights the importance of electrostatic and van der Waals interactions in the stability of the AMP-receptor complex. For example, the electrostatic interactions observed in Pleurocidin's binding to ACE2 and MMP9 are particularly significant in achieving high binding energy and stable complex formation. The correlation between electrostatic energies and binding affinity suggests that fine-tuning the charge distribution on AMPs could lead to more robust interactions, particularly with receptors containing complementary charged residues. Moreover, the matrix

Complex	HADDOCK score (a.u.)	Binding energy (kcal/mol)	Van der waals energy	Electrostatic energy	Desolvation energy	RMSD
ACE2 Complexes						
ACE2:DX600 peptide (standard inhibitor)	−76.8 +/- 0.9	−8.6	−38.7 +/- 2.9	−79.0 +/- 28.3	−26.1 +/- 4.2	1.4 +/- 0.2
ACE2:Hepcidin	−96.3 +/- 7.2	−11.3	−44.7 +/- 1.2	−250.1 +/- 24.0	−3.1 +/- 4.7	0.5 +/- 0.3
ACE2:Pleurocidin	−104.8 +/- 1.9	−11.2	−46.6 +/- 6.0	−220.6 +/- 23.5	−18.0 +/- 2.2	1.5 +/- 0.1
ACE2:Tachystatin	−102.0 +/- 3.7	−10.7	−48.4 +/- 4.4	−220.9 +/- 32.4	−20.0 +/- 4.3	1.5 +/- 0.0
ACE2:Thermolysin	−91.4 +/- 2.4	−10.7	−49.2 +/- 2.5	−131.8 +/- 20.5	−19.0 +/- 1.1	0.7 +/- 0.5
ACE2:PvHCt	−94.0 +/- 2.8	−9.9	−44.8 +/- 2.2	−117.5 +/- 15.6	−28.6 +/- 1.0	0.6 +/- 0.4
CRP Complexes						
CRP: DX600 peptide (standard inhibitor)	−90.7 +/- 8.8	−9.7	−40.8 +/- 4.6	−171.9 +/- 13.0	−15.7 +/- 2.1	0.8 +/- 0.5
CRP: Nisin	−79.3 +/- 4.1	−13.1	−43.0 +/- 4.4	−198.5 +/- 14.5	3.1 +/- 1.3	2.6 +/- 0.6
CRP: Subtilisin A	−128.1 +/- 8.3	−12.0	−46.5 +/- 6.1	−306.9 +/- 57.8	−22.6 +/- 7.6	0.6 +/- 0.5
CRP: Protegrin-1	−92.7 +/- 4.0	−11.3	−37.5 +/- 3.9	−330.3 +/- 21.8	9.7 +/- 2.4	1.3 +/- 0.1
CRP: Pardaxin	−102.4 +/- 2.9	−11.0	−50.1 +/- 0.3	−202.1 +/- 37.0	−16.5 +/- 5.7	1.7 +/- 0.2
CRP: Magainin	−108.2 +/- 5.6	−10.6	−25.2 +/- 4.2	−352.4 +/- 45.0	−14.6 +/- 1.7	1.0 +/- 0.2
MMP9 Complexes						
MMP9:DX600 peptide (standard inhibitor)	−98.3 +/- 2.5	−9.4	−55.5 +/- 3.8	−205.3 +/- 34.7	−22.0 +/- 2.3	1.4 +/- 0.3
MMP9:Tachystatin	−136.4 +/- 3.4	−12.2	−85.2 +/- 7.8	−235.8 +/- 14.4	−28.6 +/- 3.1	1.6 +/- 0.0
MMP9:Thermolysin	−114.4 +/- 3.8	−10.6	−70.3 +/- 6.6	−173.2 +/- 46.2	−27.6 +/- 3.6	1.2 +/- 0.2
MMP9:Beta-defensin 2	−93.6 +/- 4.7	−10.0	−55.2 +/- 3.8	−285.5 +/- 37.5	−3.9 +/- 1.5	0.5 +/- 0.3
MMP9:Exendin-4	−48.2 +/- 3.2	−9.8	−47.3 +/- 5.7	−55.4 +/- 20.3	−14.5 +/- 1.5	0.9 +/- 0.5
MMP9:Pleurocidin	−143.7 +/- 4.0	−9.7	−62.7 +/- 6.7	−406.5 +/- 40.9	−27.8 +/- 2.8	1.2 +/- 0.1
NLRP3 Complexes						
NLRP3:DX600 peptide (standard inhibitor)	−87.9 +/- 2.7	−10.5	−50.1 +/- 6.8	−237.3 +/- 44.7	−5.9 +/- 4.6	0.9 +/- 0.5
NLRP3:Subtilisin A	−138.7 +/- 2.8	−12.1	−75.8 +/- 4.3	−271.9 +/- 59.6	−31.2 +/- 6.0	0.7 +/- 0.4
NLRP3:Dermcidin	−98.6 +/- 14.7	−12.0	−45.9 +/- 4.1	−374.3 +/- 87.9	11.9 +/- 4.2	1.0 +/- 0.6
NLRP3:Tachystatin	−100.1 +/- 8.7	−11.3	−50.4 +/- 9.3	−281.3 +/- 36.1	−0.2 +/- 5.0	1.4 +/- 0.2
NLRP3:Thermolysin	−82.3 +/- 4.9	−11.3	−51.1 +/- 4.7	−193.6 +/- 19.4	0.3 +/- 2.8	1.2 +/- 0.9
NLRP3:Pleurocidin	−110.5 +/- 9.2	−11.0	−63.0 +/- 6.9	−253.8 +/- 21.7	−15.0 +/- 6.3	1.1 +/- 0.7
TLR4 Complexes						
TLR4:DX600 peptide (standard inhibitor)	−78.4 +/- 4.4	−12.9	−41.0 +/- 7.0	−111.4 +/- 34.1	−22.9 +/- 5.1	1.3 +/- 0.2
TLR4:Tachystatin	−125.7 +/- 2.9	−14.7	−71.8 +/- 3.2	−172.7 +/- 15.0	−23.1 +/- 2.0	0.4 +/- 0.2
TLR4:Dermcidin	−91.1 +/- 8.6	−14.3	−57.5 +/- 3.3	−137.5 +/- 37.3	−10.2 +/- 1.9	1.0 +/- 0.6
TLR4:Subtilisin A	−108.7 +/- 3.4	−13.6	−59.9 +/- 2.4	−70.5 +/- 21.6	−40.4 +/- 3.5	1.3 +/- 0.1
TLR4:Nisin	−94.6 +/- 6.3	−13.5	−55.8 +/- 5.0	−153.0 +/- 28.9	−13.6 +/- 3.1	1.3 +/- 0.1
TLR4:Chim2	−93.3 +/- 4.4	−13.3	−47.7 +/- 5.0	−119.0 +/- 23.8	−27.3 +/- 5.7	0.4 +/- 0.3

Table 1. Molecular Docking results of top 5 performing target protein-AMP complexes compared to the standard inhibitor (DX600 peptide).

reveals how structural flexibility, as indicated by RMSD values, interacts with binding energy. For instance, AMPs that form stable complexes with low RMSD values, such as Subtilisin A with NLRP3, likely maintain their active conformations in the receptor-binding pocket, contributing to their strong therapeutic potential. This information could direct future design efforts toward creating peptides that not only fit well within receptor sites but also possess the necessary structural flexibility for effective interaction. In conclusion, the correlation matrix provides a comprehensive tool for understanding how specific structural features and residue-level interactions contribute to the overall binding efficiency and stability of AMPs. By leveraging these insights, future peptide design can focus on refining key residue interactions, optimizing electrostatic and van der Waals forces, and ensuring conformational stability, ultimately improving AMP therapeutic efficacy and specificity in receptor targeting.

The correlation matrix depicted in Fig. 3 provides a detailed analysis of the interplay between different energy components—van der Waals energy, electrostatic energy, and desolvation energy—and their contributions to the binding energy of AMP-receptor complexes, specifically in receptors associated with infection-related CVDs. This matrix is essential for understanding the nuances of molecular interactions that govern the stability and affinity of AMP binding to these receptors. The correlation coefficients, ranging from −1 to 1, indicate the strength and direction of the relationships between binding energy and individual energy components. Positive values suggest a direct relationship, while negative values indicate an inverse relationship, offering valuable insights into the binding mechanisms of these AMP-receptor complexes. In the ACE2 complexes, a moderate positive correlation ($r = 0.68$) between binding energy and van der Waals energy suggests that van der Waals interactions significantly stabilize these complexes. This implies that the physical interactions between the AMP and the ACE2 receptor are primarily driven by non-covalent van der Waals forces, contributing to a strong binding affinity. In contrast, electrostatic energy ($r = 0.12$) and desolvation energy ($r = 0.31$) show much weaker correlations, indicating that these energy components have a minimal impact on the overall binding energy in ACE2 complexes. The dominance of van der Waals interactions in these complexes suggests that designing AMP-based therapies targeting ACE2 receptors for preventing infection-related CVDs should prioritize optimizing hydrophobic and steric interactions to enhance binding stability.

For the C-reactive protein (CRP) complexes, van der Waals energy ($r = 0.61$) also shows a significant positive correlation, reinforcing the importance of these interactions in maintaining strong AMP-receptor binding. However, electrostatic energy exhibits a negative correlation ($r = -0.27$), suggesting that unfavorable electrostatic interactions may slightly weaken the binding affinity. The relatively modest positive correlation for desolvation energy ($r = 0.29$) indicates that solvation effects do not play a significant role in these complexes. The results imply that, while van der Waals forces are crucial, electrostatic repulsion may limit the binding efficiency of AMPs to CRP receptors. In the case of MMP9 receptor complexes, van der Waals energy ($r = 0.39$) shows a weaker correlation with binding energy than the other receptors, suggesting a reduced contribution of hydrophobic interactions to the binding affinity. Both electrostatic energy ($r = -0.13$) and desolvation energy ($r = 0.019$) display near-zero correlations, indicating that these forces have a negligible impact on binding stability. This suggests that, for MMP9 complexes, neither van der Waals nor electrostatic interactions are particularly dominant. This may point to other factors, such as peptide conformation or flexibility, playing a more prominent role in binding affinity.

NLRP3 complexes present a more balanced interaction profile, with van der Waals energy ($r = 0.44$) and electrostatic energy ($r = 0.32$) showing moderate positive correlations. In contrast, desolvation energy ($r = -0.39$) exhibits a strong negative correlation. This indicates that while van der Waals and electrostatic interactions contribute to binding stability, desolvation effects may destabilize these complexes. The negative impact of desolvation energy could arise from the displacement of water molecules around the receptor site, destabilizing the AMP-receptor complex. Optimizing AMPs for NLRP3 could involve minimizing the unfavorable desolvation contributions while enhancing van der Waals and electrostatic interactions. Lastly, the TLR4 complexes reveal a strong positive correlation between binding energy and van der Waals energy ($r = 0.61$), similar to the ACE2 and CRP complexes. This suggests that van der Waals forces are again crucial in stabilizing the AMP-TLR4 complexes. However, electrostatic energy ($r = -0.032$) shows a near-zero correlation, indicating minimal electrostatic contributions to the overall binding energy. The desolvation energy ($r = 0.15$) exhibits a weak positive correlation, suggesting that solvation effects play a relatively minor role in these complexes.

The intermolecular contact (IC) and non-interacting surface (NIS) data in Table 2 provides a detailed assessment of the molecular interactions between receptors associated with infection-related CVDs and various AMPs, compared to the standard inhibitor DX600. This analysis highlights the unique interaction profiles of several top-performing AMPs, including Tachystatin, Thermolysin, Pleurocidin, and Subtilisin A, across different receptors such as ACE2, CRP, MMP9, NLRP3, and TLR4. These AMPs exhibit consistent binding performance, demonstrated through favorable intermolecular contacts across various energy categories and receptor sites, positioning them as potential inhibitors for preventing infection-related CVDs. For the ACE2 receptor, Pleurocidin, Tachystatin, and Thermolysin demonstrate higher charged-apolar and polar-apolar interactions than standard inhibitor DX600. Pleurocidin, with 23 charged-apolar and 11 polar-apolar contacts, indicates strong hydrophobic and polar interactions, suggesting a robust binding stability with ACE2. Tachystatin also presents significant charged-polar (9) and polar-apolar (12) interactions, enhancing its ability to form stable complexes. Thermolysin, with the highest charged-apolar interactions (29), further highlights its potential to form energetically favorable contacts with the receptor. These enhanced interactions, alongside relatively stable NIS values for all three AMPs, suggest that Pleurocidin, Tachystatin, and Thermolysin are strong candidates for inhibiting ACE2-mediated infection pathways in CVDs. Subtilisin A and Pleurocidin stand out in CRP receptor complexes with substantial intermolecular contacts. Subtilisin A exhibits 29 charged-apolar, 23 polar-apolar, and 14 apolar-apolar interactions, outperforming the standard DX600 in every category. This strong interaction profile and a high NIS apolar value (43.98) suggest that Subtilisin A can efficiently block CRP's role in infection

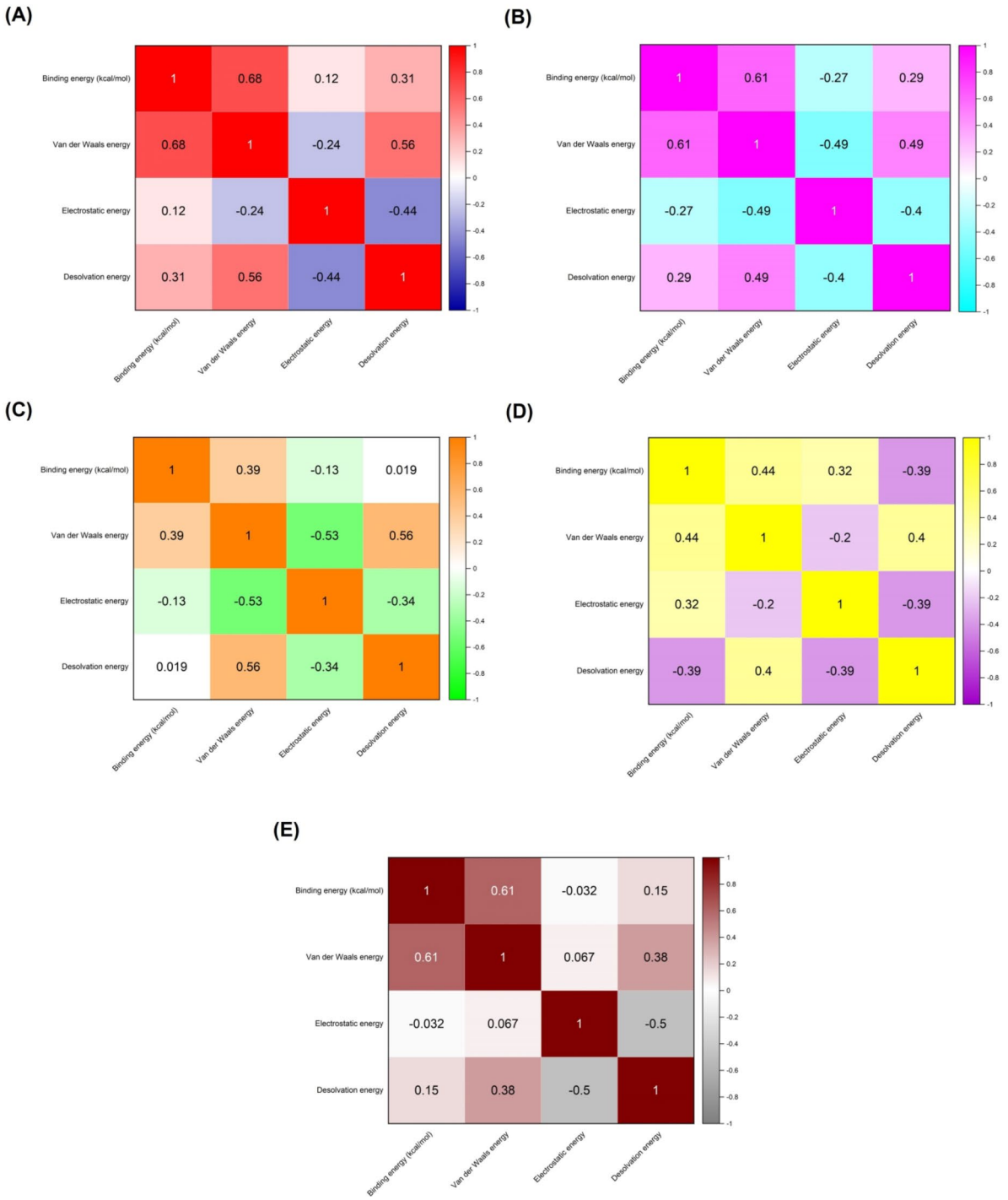

Fig. 3. Correlation matrices illustrate the relationships between binding energy (kcal/mol) and individual energy components for each target receptor-AMP complex. These include (**A**) ACE2 complexes, (**B**) CRP complexes, (**C**) MMP9 complexes, (**D**) NLRP3 complexes, and (**E**) TLR4 complexes. The matrices measure the degree of association between binding energy, van der Waals energy, electrostatic energy, and desolvation energy. The correlation values range from − 1 to 1, where 1 denotes a perfect positive correlation, −1 indicates a perfect negative correlation, and 0 signifies no correlation.

processes linked to CVDs. Pleurocidin also shows considerable binding energys, with 24 charged-apolar and 18 polar-apolar contacts, making it a competitive AMP in the CRP complex. Both peptides demonstrate high binding affinity, which could disrupt CRP's function in inflammatory responses associated with CVDs.

For the MMP9 receptor, Thermolysin and Pleurocidin again show superior performance. Thermolysin, with 29 charged-apolar and 11 polar-apolar interactions, demonstrates a clear advantage in forming hydrophobic

Complex	ICs charged-charged	ICs charged-polar	ICs charged-apolar	ICs polar-polar	ICs polar-apolar	ICs apolar-apolar	NIS charged	NIS apolar
ACE2 Complexes								
ACE2:DX600 peptide (standard inhibitor)	3	3	14	0	5	6	27.88	33.63
ACE2:Hepcidin	12	3	28	0	7	7	27.54	33.86
ACE2:Pleurocidin	8	5	23	0	11	4	27.87	34.61
ACE2:Tachystatin	5	9	20	2	12	8	26.88	33.76
ACE2:Thermolysin	4	4	29	2	9	4	27.33	34.11
ACE2:PvHCt	14	3	16	2	7	2	27.35	34.30
CRP Complexes								
CRP: DX600 peptide (standard inhibitor)	4	7	16	2	15	7	26.83	40.24
CRP: Nisin	1	3	27	1	26	19	24.71	42.35
CRP: Subtilisin A	5	4	29	4	23	14	25.9	43.98
CRP: Protegrin-1	9	11	19	0	18	11	29.03	40.00
CRP: Pardaxin	2	10	24	3	21	18	25.29	44.12
CRP: Magainin	8	5	20	2	18	10	28.12	42.50
MMP9 Complexes								
MMP9:DX600 peptide (standard inhibitor)	6	2	26	0	7	30	23.08	43.36
MMP9:Tachystatin	4	10	22	0	20	28	22.29	41.40
MMP9:Thermolysin	6	3	29	0	11	33	24.36	42.31
MMP9:Beta-defensin 2	11	3	28	0	10	24	23.33	47.33
MMP9:Exendin-4	1	4	19	0	16	22	26.06	43.66
MMP9:Pleurocidin	12	0	27	1	8	34	22.3	46.04
NLRP3 Complexes								
NLRP3:DX600 peptide (standard inhibitor)	5	7	23	2	15	8	23.84	42.36
NLRP3:Subtilisin A	1	10	37	2	19	23	23.74	44.13
NLRP3:Dermcidin	14	8	28	0	15	14	25.24	42.86
NLRP3:Tachystatin	8	11	22	5	15	11	23.99	41.14
NLRP3:Thermolysin	6	11	31	0	8	4	24	41.93
NLRP3:Pleurocidin	13	6	31	1	10	20	23.97	42.84
TLR4 Complexes								
TLR4:DX600 peptide (standard inhibitor)	4	6	15	0	23	8	24.43	30.77
TLR4:Tachystatin	5	10	24	4	26	10	23.90	31.58
TLR4:Dermcidin	10	2	26	1	21	16	25.49	33.26
TLR4:Subtilisin A	4	5	16	2	24	28	23.57	32.82
TLR4:Nisin	6	9	20	7	25	14	23.87	31.98
TLR4:Chim2	6	8	16	1	21	14	25.34	31.51

Table 2. Intermolecular contacts and non-interacting surface areas for receptors associated with infection-related CVD complexes with standard inhibitor and antimicrobial peptides. This table highlights the specific interactions and Spatial characteristics between the receptors and both the standard inhibitor (DX600 peptide) and the selected antimicrobial peptides (AMPs), aiding in the evaluation of their binding efficacy and potential therapeutic applications. Note:. • ICs: Number of intermolecular contacts. • NIS: Non-interacting surface.

interactions crucial for MMP9 inhibition. Pleurocidin, with 27 charged-apolar interactions, also shows strong binding potential, supported by this complex's highest apolar-apolar contact count (34). These AMPs outperform the standard inhibitor DX600, which has only 26 charged-apolar contacts, suggesting that Thermolysin and Pleurocidin can better interfere with MMP9's role in infection-related tissue damage in CVDs. In the NLRP3 receptor, Tachystatin, Thermolysin, and Pleurocidin again exhibit consistently strong binding characteristics. Tachystatin displays many polar-polar (5) and apolar-apolar (11) contacts, reinforcing its stability within the NLRP3 complex. Thermolysin, with 31 charged-apolar and 8 polar-apolar interactions, showcases its significant hydrophobic interaction profile, while Pleurocidin leads with the highest charged-apolar contact count (31),

emphasizing its binding efficiency. These interaction profiles indicate that these AMPs can effectively inhibit NLRP3, potentially reducing its involvement in inflammatory responses during infection-related CVDs. Finally, in TLR4 receptor complexes, Tachystatin, Subtilisin A, and Pleurocidin demonstrate strong intermolecular contacts. Tachystatin, with 24 charged-apolar and 26 polar-apolar contacts, highlights its capacity to engage with both charged and polar regions of the receptor. With 28 apolar-apolar interactions, Subtilisin A presents a solid hydrophobic binding potential. In contrast, Pleurocidin's interaction profile, including 20 charged-apolar and 25 polar-apolar contacts, shows its versatility in forming intermolecular bonds. These interactions and comparable NIS values suggest that these AMPs can effectively inhibit TLR4-mediated infection pathways, often linked to inflammation and cardiovascular complications. Detailed molecular interaction results are available in Supplementary Data 2.

Table 3 presents a detailed examination of hydrogen bond interactions between infection-related CVD receptor complexes and AMPs compared with the standard inhibitor. For the ACE2 complex, strong interactions were observed, with the shortest hydrogen bond distance being 2.58 Å between Glu23 of ACE2 and Lys24 of Hepcidin. This bond plays a critical role in stabilizing the ACE2-receptor complex, facilitating its interaction with the virus and contributing to the pathophysiology of infection-related CVDs. In the CRP complex, significant interactions include the bond between Glu147 of CRP and Lys22 of Nisin at a distance of 2.66 Å, which likely influences the receptor's ability to mediate inflammatory responses, crucial in CVD progression. MMP9 shows multiple hydrogen bonds, with a prominent bond between Glu111 of MMP9 and Leu6 of Tachystatin at 2.66 Å, indicating stable interaction. MMP9 is involved in extracellular matrix degradation, a key process in the development of vascular instability and cardiovascular diseases. Similarly, the NLRP3 A complex reveals strong binding with the shortest bond between Arg452 of NLRP3 and Glu23 of Subtilisin A, both at 2.61 Å, which might modulate inflammasome activation, thus impacting inflammation and immune response in CVDs. Finally, TLR4 interactions show consistent hydrogen bonding, particularly between His458 of TLR4 and Val12 of Tachystatin at 2.69 Å, contributing to the peptide's binding efficacy. TLR4 activation is known to trigger immune responses, including inflammation, which is implicated in atherosclerosis and other CVDs. These hydrogen bonds indicate that the antimicrobial peptides, particularly Tachystatin and Subtilisin A, form strong and stable interactions with their respective receptors, comparable to or exceeding the standard inhibitor, and could help modulate the key pathways involved in infection and CVD progression.

The results demonstrate that the AMPs outperform the standard inhibitor DX600 in terms of binding affinity and stability across various receptor complexes. This is significant because it suggests that AMPs may offer several therapeutic advantages over traditional inhibitors in treating infection-related CVDs. For instance, the higher binding affinities of AMPs, such as Tachystatin, Pleurocidin, and Subtilisin A, compared to DX600, indicate that these peptides may form stronger, more stable interactions with their target receptors. This could enhance their ability to inhibit receptor-mediated signaling pathways involved in inflammation, infection, and vascular instability, all of which contribute to CVD progression. Additionally, the stability of these peptides under physiological conditions, as reflected in their favorable electrostatic and van der Waals energies, suggests that they may remain active in the bloodstream longer than traditional small-molecule inhibitors, which are often subject to rapid degradation and clearance. Moreover, the superior binding of these AMPs to key receptors implicated in CVDs, such as ACE2, MMP9, and TLR4, positions them as promising candidates for targeted therapeutic interventions. By effectively modulating these receptor functions, AMPs could prevent the degradation of the extracellular matrix, mitigate inflammation, and interfere with the viral entry mechanisms, thereby providing a multi-faceted approach to combating infections associated with CVDs. In contrast, DX600, a standard inhibitor, may not offer the same level of specificity or stability, limiting its effectiveness in clinical settings. The enhanced binding properties and stability of AMPs make them an attractive alternative for the development of novel therapeutic agents aimed at preventing or treating infection-related cardiovascular diseases.

Molecular dynamics (MD) simulations

Table 4 overviews the time-averaged structural properties obtained from molecular dynamics (MD) simulations of target receptor-AMP complexes. The data reveal that Tachystatin, Thermolysin, Pleurocidin, and Subtilisin A exhibit significant structural stability and binding characteristics compared to the standard inhibitor, DX600 peptide, across various receptors associated with infection-related CVDs. For ACE2 complexes, Tachystatin shows a lower average RMSD (3.527 Å) (Fig. 4A) and average RMSF (0.747 Å) compared to the standard inhibitor DX600 peptide (RMSD: 3.659 Å, RMSF: 0.792 Å), indicating a slight decrease in conformational fluctuations and structural deviation. However, Tachystatin has the highest average number of hydrogen bonds (53) and the most favorable potential energy (−660,317.634 kcal/mol), suggesting that it forms more stable and energetically favorable interactions with ACE2 than DX600 peptide.

In CRP complexes, Subtilisin A and Pleurocidin display better structural stability with average RMSD values of 1.977 Å and 2.313 Å, respectively, compared to the standard inhibitor DX600 peptide (2.402 Å). Subtilisin A also has a comparable number of hydrogen bonds (16) and lower potential energy (−166,979.914 kcal/mol) than DX600 peptide (−184,719.286 kcal/mol), indicating efficient binding and favorable energetics. Pleurocidin exhibits a similar number of hydrogen bonds (16) and lower potential energy (−143,351.144 kcal/mol) than the DX600 peptide. For MMP9 complexes, Tachystatin and Thermolysin demonstrate lower average RMSD values (2.209 Å and 1.992 Å, respectively) compared to the standard inhibitor DX600 peptide (2.555 Å), indicating better structural stability. Tachystatin has a higher average number of hydrogen bonds (13) and more favorable potential energy (−195,363.451 kcal/mol) compared to DX600 peptide (−164,237.839 kcal/mol), suggesting that Tachystatin provides more stable and energetically favorable interactions with MMP9. In NLRP3 complexes, Tachystatin and Subtilisin A exhibit better structural stability with average RMSD values of 3.359 Å and 3.521 Å, respectively, compared to the standard inhibitor DX600 peptide (3.636 Å) (Fig. 4B). Tachystatin also shows a higher number of hydrogen bonds (49) and the most favorable potential energy (−1,467,888.897 kcal/mol)

Complex	Residue (Receptor)	Protein Atom (Receptor)	Residue (Interacting Peptide)	Protein Atom (Interacting Peptide)	Interaction Distance (Å)
ACE2:Hepcidin	Ser19	OG	Lys24	NZ	2.81
	Glu23	OE2	Lys24	NZ	2.58
	Asp30	OD1	Arg16	NH1	2.71
	Asp30	OD2	Arg16	NH2	2.59
	Asp38	OD2	Lys18	NZ	2.61
CRP: Nisin	Asn61	OD1	Cys19	SG	2.94
	Glu147	OE1	Lys22	NZ	2.66
	Glu147	OE2	Asn20	ND2	2.93
	Gln150	NE2	Gly18	O	2.97
	Gln150	NE2	Cys19	O	2.86
MMP9:Tachystatin	Glu111	OE2	Leu6	N	2.66
	Tyr179	OH	Arg3	NE	2.90
	Pro180	O	Thr20	OG1	2.64
	Asp182	O	Arg14	NH2	2.79
	Gly183	O	Arg14	NH1	2.88
	Asp185	O	Arg14	NH1	2.81
	Leu188	N	Tyr38	OH	2.85
	Gln199	OE1	Arg3	NH1	3.11
	Gln199	OE1	Arg3	NH2	2.93
	Tyr393	OH	Thr37	OG1	2.89
	His411	O	Arg40	NH2	2.86
	His411	ND1	Asn10	N	3.27
	Ser412	O	Arg40	NH1	3.28
	Ser412	O	Arg40	NH2	2.75
NLRP3:Subtilisin A	Gln147	OE1	Lys2	NZ	2.70
	Glu150	OE2	Ala5	N	2.95
	Glu150	OE2	Thr6	N	3.17
	Glu150	OE2	Cys7	SG	2.95
	Lys164	O	Trp34	NE1	2.77
	Glu425	OE2	Cys13	N	2.68
	Arg452	NE	Glu23	OE2	2.61
	Arg452	NH2	Glu23	OE1	2.61
	Arg502	NH1	Thr6	O	2.78
TLR4:Tachystatin	Asn383	O	Arg30	NH1	3.27
	Asn383	O	Arg30	NH2	2.94
	Ser386	O	Tyr44	OH	2.78
	Lys435	NZ	Cys23	O	2.74
	Lys435	NZ	Cys24	O	2.94
	Lys435	NZ	Leu27	O	2.71
	His458	NE2	Val12	O	2.69
	Arg460	NH2	Gly17	O	2.73

Table 3. Detailed examination of hydrogen bond interactions between receptors associated with infection-related CVD complexes with standard inhibitor and antimicrobial peptides.

among the peptides tested, indicating that it forms highly stable and energetically favorable interactions with NLRP3 compared to DX600 peptide. Finally, in TLR4 complexes, Tachystatin and Subtilisin A have lower average RMSD values (2.914 Å and 3.106 Å) compared to the standard inhibitor DX600 peptide (2.968 Å). Tachystatin also exhibits a higher number of hydrogen bonds (46) and more favorable potential energy (−780,309.925 kcal/mol) than DX600 peptide (−755,432.195 kcal/mol), suggesting that Tachystatin provides a more stable and energetically favorable binding interaction with TLR4.

RMSF values offer a detailed view of residue flexibility within receptors associated with infection-related CVD-AMP complexes, as depicted in Fig. 5. The results indicate that the AMPs exhibit a significant correspondence with the standard inhibitor, DX600 peptide, regarding residue flexibility, suggesting that these AMPs can disrupt receptor stability similarly to the standard inhibitor. The ACE2 complexes' RMSF patterns of Pleurocidin, Tachystatin, and Thermolysin closely resemble those of the standard inhibitor, particularly within residues Asn330 to Asp355. In CRP complexes, the RMSF values of these AMPs show a strong correlation with

Complex	Average RMSD (Å)	Average RMSF (Å)	Average RoG (Å)	Number of hydrogen bonds between the two proteins	Potential energy (kcal/mol)
ACE2 Complexes					
ACE2 (apo-protein)	3.281	0.772	2.501	N/A	−440,543.758
ACE2:DX600 peptide (standard inhibitor)	3.659	0.792	2.597	50	−583,916.418
ACE2:Hepcidin	3.645	0.822	2.548	49	−477,259.112
ACE2:Pleurocidin	3.518	0.791	2.572	50	−466,473.033
ACE2:Tachystatin	3.527	0.747	2.658	53	−660,317.634
ACE2:Thermolysin	3.440	0.789	2.703	54	−572,443.081
ACE2:PvHCt	3.493	0.795	2.614	51	−603,748.294
CRP Complexes					
CRP (apo-protein)	2.010	0.726	1.608	N/A	−136,101.530
CRP: DX600 peptide (standard inhibitor)	2.402	0.958	1.735	14	−184,719.286
CRP: Nisin	2.313	0.787	1.737	16	−288,567.674
CRP: Subtilisin A	1.977	0.757	1.704	16	−166,979.914
CRP: Protegrin-1	2.416	0.951	1.653	17	−179,352.210
CRP: Pardaxin	2.355	0.864	1.687	16	−143,351.144
CRP: Magainin	2.192	0.814	1.688	17	−145,486.514
MMP9 Complexes					
MMP9 (apo-protein)	2.078	1.094	1.495	N/A	−111,366.323
MMP9:DX600 peptide (standard inhibitor)	2.555	1.267	1.610	11	−164,237.839
MMP9:Tachystatin	2.209	1.359	1.631	13	−195,363.451
MMP9:Thermolysin	1.992	1.295	1.666	15	−131,816.946
MMP9:Beta-defensin 2	2.498	1.330	1.641	13	−163,272.695
MMP9:Exendin-4	2.820	1.461	1.661	12	−191,827.586
MMP9:Pleurocidin	2.274	1.095	1.573	11	−119,726.773
NLRP3 Complexes					
NLRP3 (apo-protein)	3.276	0.924	3.614	N/A	−900,750.476
NLRP3:DX600 peptide (standard inhibitor)	3.636	1.056	3.652	45	−1,127,743.577
NLRP3:Subtilisin A	3.521	1.044	3.667	48	−1,070,921.883
NLRP3:Dermcidin	3.501	1.048	3.728	50	−1,370,475.374
NLRP3:Tachystatin	3.359	0.972	3.678	49	−1,467,888.897
NLRP3:Thermolysin	3.262	0.941	3.638	53	−1,239,438.186
NLRP3:Pleurocidin	3.207	1.051	3.587	49	−977,382.530
TLR4 Complexes					
TLR4 (apo-protein)	2.642	0.720	3.201	N/A	−718,765.881
TLR4:DX600 peptide (standard inhibitor)	2.968	0.775	3.268	38	−755,432.195
TLR4:Tachystatin	2.914	0.878	3.221	46	−780,309.925
TLR4:Dermcidin	2.938	0.900	3.234	43	−708,531.477
TLR4:Subtilisin A	3.106	0.831	3.194	45	−711,005.102
TLR4:Nisin	2.962	0.815	3.193	44	−712,561.934
TLR4:Chim2	3.143	0.918	3.220	45	−743,878.601

Table 4. Time-averaged structural properties obtained from the MD simulations of target receptor-AMP complexes.

the standard inhibitor around residues Ala55 to Ile65 and Glu130 to Asp155. For MMP9 complexes, the RMSF profiles of Pleurocidin, Tachystatin, and Thermolysin match those of the standard inhibitor in residues Ile125 to Asp138. In the NLRP3 and TLR4 complexes, the RMSF values of the AMPs align closely with those of the standard inhibitor in crucial binding regions, including residues Ser161 to His175 and Lys375 to Asn400 for NLRP3, and Ser360 to Leu380 and Gln510 to Leu535 for TLR4. Overall, the RMSF data highlight that the AMPs can disrupt receptor stability in a manner similar to the standard inhibitor. The ability of these AMPs to induce comparable flexibility in critical binding regions underscores their potential as effective disruptors of receptor stability, akin to the DX600 peptide.

Molecular mechanics/poisson–boltzmann surface area (MM/PBSA) calculations

The binding affinities of selected AMPs for target receptors were assessed using MM/PBSA calculations (based on the MD simulation), with results in Table 5. Among the peptides evaluated, Tachystatin, Pleurocidin, and Subtilisin A emerged as the most consistent in exhibiting favorable binding energies. For ACE2 complexes,

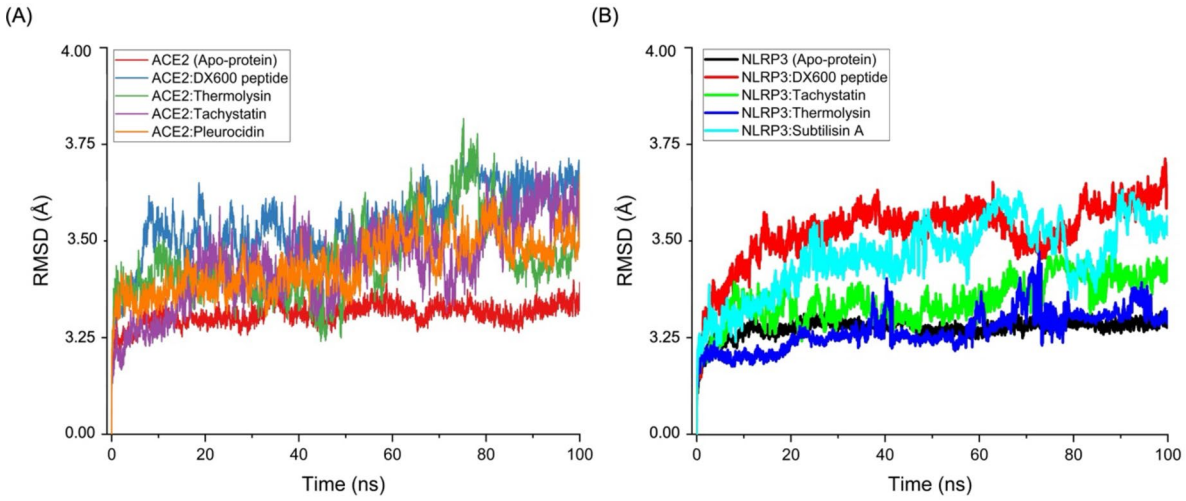

Fig. 4. Molecular dynamics (MD) simulation results showing the Root Mean Square Deviation (RMSD) profiles for different complexes: (**A**) ACE2 complexes and (**B**) NLRP3 complexes, highlighting their structural stability and dynamic behavior over time.

Tachystatin stands out with an average binding energy of −61.58 kcal/mol, significantly more favorable than the standard inhibitor DX600 peptide, which has an average binding energy of −22.28 kcal/mol. Pleurocidin also shows strong binding with an average energy of −46.58 kcal/mol, while Subtilisin A's binding affinity is slightly less favorable at −44.82 kcal/mol. These results suggest that Tachystatin and Pleurocidin exhibit superior binding capabilities compared to the standard inhibitor, with Tachystatin showing the most significant potential. In CRP complexes, Subtilisin A exhibits the most favorable binding energy with an average of −70.71 kcal/mol, followed by Protegrin-1 at −67.56 kcal/mol and Nisin at −38.73 kcal/mol. This contrasts with the standard inhibitor DX600 peptide, which has an average binding energy of −27.99 kcal/mol. The superior binding energy of Subtilisin A and Protegrin-1 in CRP complexes underscores their effectiveness compared to the standard inhibitor.

For MMP9 complexes, Tachystatin again demonstrates the highest binding affinity with an average energy of −96.61 kcal/mol, followed closely by Pleurocidin at −94.24 kcal/mol. These values are significantly lower (more favorable) than the standard inhibitor DX600 peptide, which has an average energy of −52.61 kcal/mol. The binding energies of Tachystatin and Pleurocidin indicate their strong interaction with MMP9, surpassing that of the standard inhibitor. In NLRP3 complexes, Subtilisin A and Tachystatin exhibit comparable binding affinities with averages of −71.12 kcal/mol and −69.20 kcal/mol, respectively, outperforming the standard inhibitor DX600 peptide, which has an average of −44.35 kcal/mol. This highlights the superior binding potential of Subtilisin A and Tachystatin for NLRP3. Finally, in TLR4 complexes, Tachystatin displays a favorable binding energy of −59.69 kcal/mol, more favorable than the standard inhibitor DX600 peptide, with an average energy of −32.82 kcal/mol. Subtilisin A's average binding energy is −43.24 kcal/mol, indicating that it also binds effectively, though less so than Tachystatin. For Tachystatin, the residues Arg3, Phe9, Asn10, Arg14, and Arg3 were found to have the lowest binding affinity, with all values below −4.0 kcal/mol. These residues play a significant role in the interaction profile of Tachystatin, contributing to the overall stability of the complex. Their interactions with the AMP could provide insights into potential areas for optimization in future therapeutic applications. For Pleurocidin, the residues His11, Lys14, Leu21, and Tyr24 were identified as having the lowest binding affinities, with all values also falling below −4.0 kcal/mol. These residues are critical to the interaction between Pleurocidin and its target receptor, affecting the binding affinity and stability of the complex.

Haemolytic activity prediction of antimicrobial peptides (AMPs)

The DX600 peptide, which serves as the standard inhibitor in this study, exhibited a very low PROB score of 0.004, indicating a strong likelihood of being non-hemolytic. This suggests that DX600 may be a safer therapeutic candidate when considering the potential for hemolysis, particularly in clinical settings. In contrast, several peptides, such as Beta-defensin 2 (PROB = 0.967), Chim2 (PROB = 0.973), and Pardaxin (PROB = 0.988), showed significantly higher PROB scores, indicating a substantial risk of hemolytic activity. This finding raises important considerations for their therapeutic application, as hemolytic peptides may lead to adverse effects in vivo, potentially limiting their clinical utility. Among the AMPS evaluated, Tachystatin, Thermolysin, Pleurocidin, and Subtilisin A emerged as the most promising candidates based on their molecular docking and MD simulations, alongside their relatively low PROB scores, indicating a lower risk of hemolysis (Table 6). Tachystatin demonstrated a PROB score of 0.576, which indicates a moderate risk of hemolytic activity. Although its PROB score is higher than that of DX600, it remains significantly lower than many other peptides tested, such as Beta-defensin 2, Chim2, and Pardaxin. Thermolysin exhibited a PROB score of 0.288, suggesting a lower likelihood of hemolytic activity compared to several other peptides. Pleurocidin, with a PROB score of 0.095, displayed the lowest potential for hemolysis among the evaluated peptides. Subtilisin A, with a PROB

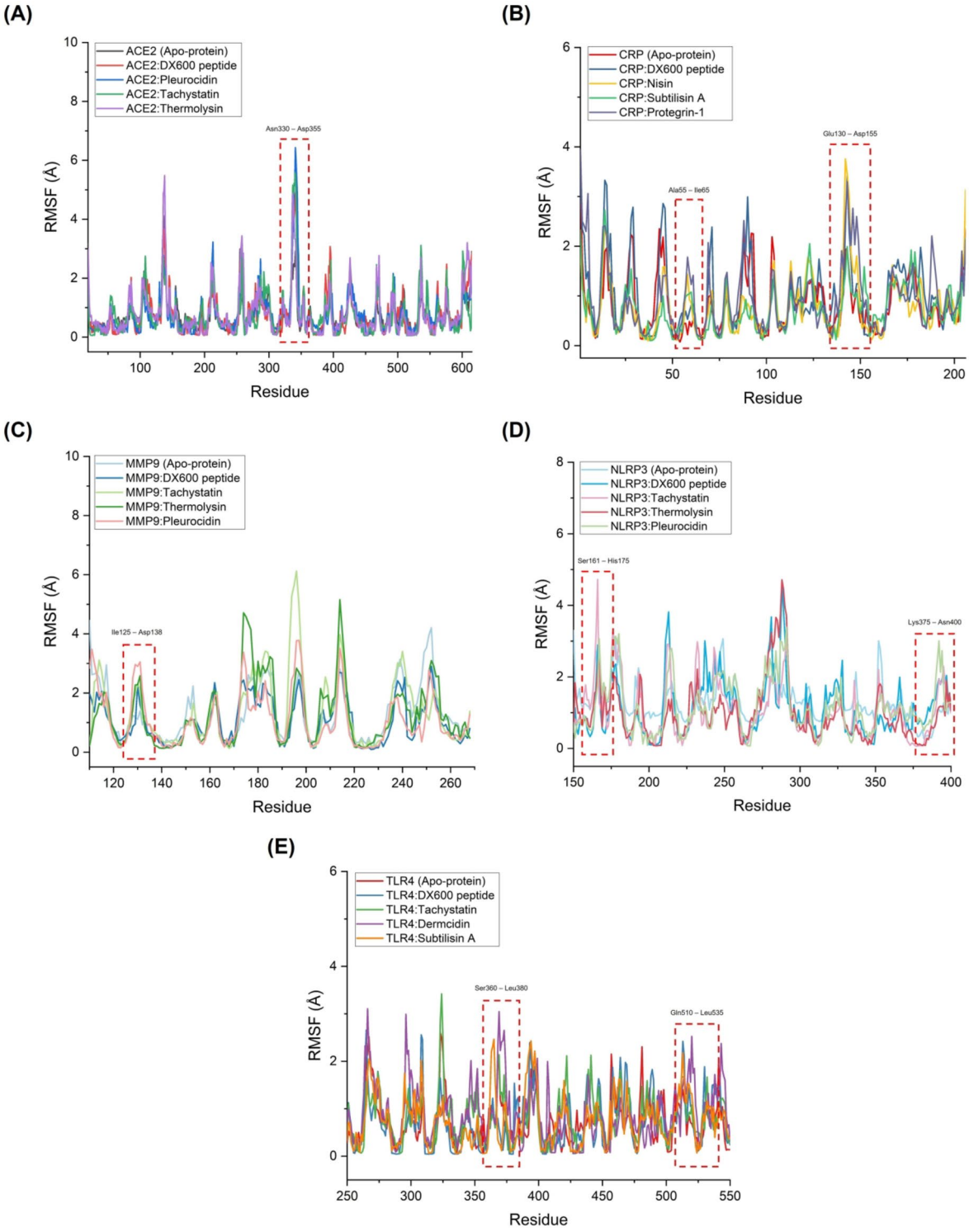

Fig. 5. Molecular dynamics (MD) simulation results illustrating the Root Mean Square Fluctuation (RMSF) profiles, highlighting the flexibility of residues within different complexes: (**A**) ACE2 complexes, (**B**) CRP complexes, (**C**) MMP9 complexes, (**D**) NLRP3 complexes, and (**E**) TLR4 complexes.

score of 0.049, also showed a very low likelihood of hemolytic activity. Despite Tachystatin's relatively higher PROB score compared to the standard peptide, its favorable interaction profiles and stability in complexes with target receptors, along with a moderate hemolytic risk, suggest that it could still be a viable candidate for further development, especially when considering its strong binding affinity and stability in receptor complexes. Furthermore, Tachystatin's therapeutic potential goes beyond just its hemolytic activity. It demonstrates strong binding affinity and stability in complex with infection-related CVD receptors, as shown in our molecular

Complex	MM/PBSA calculation results $\Delta G_{binding}$ (kcal/mol)			Average (kcal/mol)
	I	II	III	
ACE2 Complexes				
ACE2:DX600 peptide (standard inhibitor)	−22.07	−22.51	−22.27	−22.28
ACE2:Hepcidin	−53.81	−53.35	−52.56	−53.24
ACE2:Pleurocidin	−46.94	−46.17	−46.64	−46.58
ACE2:Tachystatin	−62.34	−60.47	−61.93	−61.58
ACE2:Thermolysin	−44.14	−45.63	−44.70	−44.82
ACE2:PvHCt	−31.42	−31.08	−31.18	−31.22
CRP Complexes				
CRP: DX600 peptide (standard inhibitor)	−28.23	−27.82	−27.93	−27.99
CRP: Nisin	−38.81	−38.65	−38.75	−38.73
CRP: Subtilisin A	−70.24	−70.99	−70.92	−70.71
CRP: Protegrin-1	−67.52	−67.86	−67.31	−67.56
CRP: Pardaxin	−60.72	−56.91	−60.72	−59.45
CRP: Magainin	−53.41	−53.47	−53.35	−53.41
MMP9 Complexes				
MMP9:DX600 peptide (standard inhibitor)	−53.14	−53.07	−51.63	−52.61
MMP9:Tachystatin	−96.59	−96.7	−96.55	−96.61
MMP9:Thermolysin	−66.02	−68.04	−65.97	−66.67
MMP9:Beta-defensin 2	−78.69	−78.72	−77.75	−78.38
MMP9:Exendin-4	−23.95	−23.51	−23.60	−23.68
MMP9:Pleurocidin	−94.82	−94.15	−93.77	−94.24
NLRP3 Complexes				
NLRP3:DX600 peptide (standard inhibitor)	−43.87	−45.63	−43.57	−44.35
NLRP3:Subtilisin A	−69.45	−71.10	−72.81	−71.12
NLRP3:Dermcidin	−61.90	−62.54	−62.43	−62.29
NLRP3:Tachystatin	−69.04	−69.56	−69.02	−69.20
NLRP3:Thermolysin	−28.14	−28.87	−28.77	−28.59
NLRP3:Pleurocidin	−60.13	−55.24	−60.83	−58.73
TLR4 Complexes				
TLR4:DX600 peptide (standard inhibitor)	−33.05	−32.48	−32.93	−32.82
TLR4:Tachystatin	−59.73	−59.72	−59.62	−59.69
TLR4:Dermcidin	−45.92	−46.23	−44.51	−45.55
TLR4:Subtilisin A	−43.62	−42.51	−43.61	−43.24
TLR4:Nisin	−56.90	−57.13	−56.90	−56.97
TLR4:Chim2	−57.95	−58.19	−58.45	−58.19

Table 5. Time-averaged structural properties obtained from the MD simulations of target receptor-AMP complexes.

docking and MD simulation results. These favorable interaction profiles, along with its stability in receptor complexes, suggest that Tachystatin could be a viable therapeutic candidate with potential for optimization. Additionally, the hemolytic risk can be further addressed through structural modifications, such as peptide engineering or formulation strategies, to mitigate its hemolytic activity while maintaining its therapeutic efficacy.

Physicochemical characterization of antimicrobial peptides (AMPs)

The physicochemical analysis of AMPs provides valuable insights into their stability, solubility, and potential biological activity (Table 8). Among the peptides analyzed, Tachystatin, Pleurocidin, and Subtilisin A emerged as three of the best-performing candidates based on their favorable physicochemical properties. Tachystatin exhibited a theoretical isoelectric point (pI) of 9.18, an extinction coefficient of 7,825 M^{-1} cm^{-1}, a long-estimated half-life of 30.0 h, an aliphatic index of 81.49, and a stable instability index of 32.98. Pleurocidin also demonstrated stability, with an instability index of 4.97, a pI of 10.18, an extinction coefficient of 6,990 M^{-1} cm^{-1}, and a high half-life of 30.0 h. Similarly, Subtilisin A exhibited a stable instability index of 24.71, a pI of 4.03, an extinction coefficient of 5,625 M^{-1} cm^{-1}, and a reasonable half-life of 1.4 h. The instability index plays a crucial role in determining peptide stability, where values ≤ 40.00 classify peptides as stable and those > 40.00 as unstable. Among the peptides studied, several exhibited remarkable stabilities, including Tachystatin (32.98), Pleurocidin (4.97), and Subtilisin A (24.71). These peptides are likely to maintain structural integrity, which

Antimicrobial peptide	Sequence	nTer	cTer	PROB
DX600 peptide (standard inhibitor)	GDYSHCSPLRYYPWWKCTYPDPEGGG	None	None	0.004
Aurein	GLFDIIKKIAESF	None	None	0.779
Beta-defensin 2	MRVLYLLFSFLFIFLMPLPGVFGGIGDPVTCLKSGAICHPVFCPRRYKQIGTCGLPGTKCCKKP	None	None	0.967
Bombinin	IIGPVLGLVGSALGGLLKKIG	None	None	0.742
Cathelicidin	LLGDFFRKSKEKIGKEFKRIVQRIKDFLRNLVPRTES	None	None	0.258
Cecropin	KWKLFKKIGKFLHSAKKF	None	None	0.050
Chim2	KWAVKIIRKFIKGFISGGKRWKYM	None	None	0.973
Dermcidin	SSLLEKGLDGAKKAVGGLGKLGKDAVEDLESVGKGAVHDVKDVLDSVL	None	None	0.001
Esculentin	GIFSKLAGKKIKNLLISGLKNVGKEVGMDVVRTGIDIAGCKIKGEC	None	None	0.166
Exendin-4	DLSKQMEEEAVRLFIEWLKNGGPSSGA	None	None	0.007
Hepcidin	HFPICIFCCGCCHRSKCGMCCK	None	None	0.026
Hs05	LMGLFNRIIRKVVKLFN	None	None	0.961
Indolicidin	ILAWKWAWWAWRR	None	None	0.958
Lactoferrin	FKCRRWQWRMKKLGAPSITCVRRAF	None	None	0.001
Lavracin	WDPYFAGVKKLTKAILAVRA	None	None	0.107
Magainin	GIGKFLHSAKKFGKAFVGEIMNS	None	None	0.820
Melittin	MKFLVNVALVFMVVYISYIYAAPEPEPAPEPEAEADAEADPEAGIGAVLKVLTTGLPALISWIKRKRQQG	None	None	0.450
Microcin J25	GGAGHVPEYFVGIGTPISFYG	None	None	0.002
Nisin	MSTKDFNLDLVSVSKKDSGASPRITSISLCTPGCKTGALMGCNMKTATCNCSIHVSK	None	None	0.006
Pardaxin	GFFALIPKIISSPLFKTLLSAVGSALSSSGGQE	None	None	0.988
Piscidin	FIHHIFRGIVHAGRSIGRFLTG	None	None	0.343
Pleurocidin	GWGSFFKKAAHVGKHVGKAALTHYL	None	None	0.095
Polyphemusin I	RRWCFRVCYRGFCYRKCR	None	None	0.867
Protegrin-1	RGGRLCYCRRRFCVCVGR	None	None	0.911
PvHCt	FQDLPNFGHIQVKVFNHGEHIHH	None	None	0.272
Subtilisin A	NKGCATCSIGAACLVDGPIPDFEIAGATGLFGLWG	None	None	0.049
Tachyplesin-1	KWCFRVCYRGICYRRCR	None	None	0.663
Tachystatin	MKLQNTLILIGCLFLMGAMIGDAYSRCQLQGFNCVVRSYGLPTIPCCRGLTCRSYFPGSTYGRCQRY	None	None	0.576
Temporin-L	FVQWFSKFLGRIL	None	None	0.993
Thanatin	GSKKPVPIIYCNRRTGKCQRM	None	None	0.001
Thermolysin	GIGRDKLGKIFYRALTQYLTPTSNFSQLRAAAVQSATDLYGSTSQEVASVKQAFDAVGV	None	None	0.288

Table 6. Haemolytic activity prediction of selected amps. The table presents the antimicrobial peptides' sequences and their corresponding PROB scores, which indicate their likelihood of causing haemolysis; lower scores suggest a reduced potential for toxicity. Note: The PROB score is a normalized sigmoid value that ranges from 0 to 1. A score of 0 indicates a high likelihood of being non-hemolytic, while a score of 1 suggests a high likelihood of being hemolytic. nTer is the N-terminal of a peptide, indicating the beginning of the peptide chain, which has a free amino group ($-NH_2$). cTer is the C-terminal of a peptide, indicating the end of the peptide chain, which has a free carboxyl group (-COOH).

is critical for their function as antimicrobial agents. In contrast, highly unstable peptides, such as Lactoferrin (77.92), DX600 (69.97), and Exendin-4 (64.81), may degrade more rapidly in biological environments, limiting their potential as effective therapeutic agents.

Apart from stability, hydrophobicity, aliphatic index, and extinction coefficients contribute to the potential efficacy of AMPs. Tachystatin and Pleurocidin demonstrated moderate hydropathicity values of 0.240 and − 0.068, respectively, indicating balanced hydrophobic and hydrophilic characteristics, which are essential for membrane interaction. Subtilisin A, with a hydropathicity value of 0.691, also exhibited a favorable balance. Additionally, the high aliphatic index of Tachystatin (81.49), Pleurocidin (70.40), and Subtilisin A (89.43) suggests good thermal stability, enhancing their potential use in various biomedical applications.

Discussion

Key findings from molecular simulations and their correlation with other research

The molecular docking and dynamics simulations conducted in this study provided significant insights into the interactions between AMPs and receptors implicated in infection-related CVDs. These findings highlight the potential of AMPs as therapeutic agents and contribute to our understanding of their binding mechanisms and stability compared to conventional inhibitors. Our simulations highlight that several AMPs—Tachystatin, Thermolysin, Pleurocidin, and Subtilisin A—demonstrate significant binding affinity towards key receptors such as ACE2, MMP9, CRP, NLRP3, and TLR4. These peptides exhibited strong binding interactions, as indicated by favorable HADDOCK scores and binding energies. Notably, Tachystatin and Thermolysin showed particularly

Antimicrobial peptide	Theoretical pI	Extinction coefficients*	Estimated half-life**	Instability index	Aliphatic index	GRAVY***
DX600 peptide (standard inhibitor)	5.38	17,085	30.0 h	69.97	15.00	−1.177
Aurein	6.07	NV	30.0 h	20.48	127.69	0.669
Beta-defensin 2	9.46	3355	30.0 h	41.32	92.81	0.605
Bombinin	10.00	NV	20.0 h	12.44	180.95	1.433
Cathelicidin	10.61	NV	5.5 h	23.34	89.46	−0.724
Cecropin	10.78	5500	1.3 h	−13.06	70.56	−0.572
Chim2	11.30	12,490	1.3 h	48.87	81.25	−0.250
Dermcidin	5.07	NV	1.9 h	10.12	115.63	−0.029
Esculentin	9.63	125	30.0 h	−8.14	114.35	0.220
Exendin-4	4.59	5500	1.1 h	64.81	75.93	−0.537
Hepcidin	8.53	500	3.5 h	48.38	35.45	0.664
Hs05	12.02	NV	5.5 h	−2.27	148.82	0.712
Indolicidin	12.01	27,500	20.0 h	44.98	83.08	−0.285
Lactoferrin	11.84	11,125	1.1 h	77.92	50.80	−0.576
Lavracin	10.00	6990	2.8 h	13.44	107.50	0.295
Magainin	10.00	NV	30.0 h	−0.10	72.17	0.083
Melittin	4.69	9970	30.0 h	51.70	106.00	0.239
Microcin J25	5.24	2980	30.0 h	28.16	69.52	0.400
Nisin	8.99	250	30.0 h	28.89	68.42	−0.011
Pardaxin	8.59	NV	30.0 h	39.52	112.42	0.745
Piscidin	12.30	NV	1.1 h	39.66	106.36	0.455
Pleurocidin	10.18	6990	30.0 h	4.97	70.40	−0.068
Polyphemusin I	10.33	8730	1.0 h	49.58	16.11	−0.833
Protegrin-1	10.66	1740	1.0 h	62.13	53.89	−0.250
PvHCt	6.54	NV	1.1 h	44.07	76.09	−0.596
Subtilisin A	4.03	5625	1.4 h	24.71	89.43	0.691
Tachyplesin-1	9.93	8730	1.3 h	13.22	40.00	−0.518
Tachystatin	9.18	7825	30.0 h	32.98	81.49	0.240
Temporin-L	11.00	5500	1.1 h	24.05	112.31	0.823
Thanatin	10.47	1615	30.0 h	39.88	50.95	−0.900
Thermolysin	9.31	4470	30.0 h	23.44	84.41	−0.071

Table 7. Physicochemical properties of antimicrobial peptides (AMPs), including stability, hydrophobicity, and half-life predictions. * Extinction coefficients are in units of M^{-1} cm^{-1}, at 280 nm measured in water. NV = not visible by UV spectrophotometry due to lack of Trp, Tyr, or Cys. ** Mammalian reticulocytes, in vitro. *** Grand average of hydropathicity.

Receptors associated with infection-related CVDs	PDB ID	Active site (Number of residues)	Ref
Angiotensin-Converting Enzyme 2 (ACE2)	6M0J	24, 30, 35, 38, 41, 42, 83, 353	84
C-reactive protein (CRP)	1B09	58, 60, 61, 66, 74, 81, 138, 139, 140, 147, 150	85
Matrix Metalloproteinase-9 (MMP9)	1GKC	131, 149, 165, 175, 177, 182, 183, 185, 186, 187, 188, 189, 190, 197, 199, 201, 203, 205, 206, 208, 211 ,212, 213, 214, 215, 393, 401, 402, 405, 421, 422, 423	86
NLRP3 Inflammasome	6NPY	165, 166, 167, 229, 230, 231, 232, 379, 411, 414, 520	87
Toll-Like Receptor-4 (TLR4)	3FXI	363, 364, 365, 386, 409, 410, 411, 433, 458, 507, 533	88

Table 8. Overview of target receptors related to infection-related cardiovascular diseases. It includes the protein data bank (PDB) IDs for each receptor and details their respective active sites, which are critical for Understanding potential interactions with antimicrobial peptides (AMPs).

strong binding with ACE2, and Pleurocidin performed well with multiple receptors, including ACE2 and MMP9. These findings are consistent with previous studies that have demonstrated the potential of AMPs to modulate receptor activity in various disease contexts[39,40]. In relation to prior research, Tachystatin's superior binding affinity for ACE2 aligns with a finding that peptides targeting ACE2 could modulate its activity and influence cardiovascular disease outcomes[41]. Similarly, the strong binding of Thermolysin and Pleurocidin to MMP9 and CRP reflects their potential to target inflammation-related pathways. These corroborating studies emphasize the role of peptides in controlling matrix metalloproteinase activity and inflammatory responses[19,42,43]. MD

simulations provided insights into the stability and conformational dynamics of AMP-receptor complexes. Tachystatin and Pleurocidin, in particular, displayed favorable structural stability with lower RMSD and RMSF values compared to the standard inhibitor DX600. These observations are supported by previous studies showing the importance of peptide stability in maintaining therapeutic efficacy[44–46]. The consistent hydrogen bonding patterns and favorable potential energies observed in our simulations underscore the potential of these AMPs to form stable and energetically favorable interactions with their targets. Furthermore, our results suggest that van der Waals interactions are crucial for binding stability, as corroborated by studies that emphasize the role of non-covalent interactions in peptide-receptor binding[47,48]. The significance of this study lies in its novel exploration of AMP-based modulation of receptor activity in infection-driven CVDs. While AMPs have been primarily studied for their antimicrobial properties, their ability to modulate critical receptors involved in cardiovascular disease progression has not been thoroughly investigated. This study expands the knowledge of AMPs by demonstrating their potential to interact with and modulate CVD-related receptors such as ACE2, MMP9, CRP, NLRP3, and TLR4. These interactions may help manage infections and regulate inflammation and immune responses involved in CVDs, thus providing a dual therapeutic benefit. The findings of this study contribute to our understanding of AMPs beyond their antimicrobial properties, suggesting they may play a role in modulating infection and inflammation in cardiovascular diseases. This expands the potential applications of AMPs as therapeutic agents targeting infection-driven CVDs.

Moreover, we conducted a toxicity assessment through haemolytic activity prediction using the HAPPENN tool, which leverages advanced neural network algorithms to predict the potential for hemolytic activity in therapeutic peptides. This analysis provided valuable insights into the safety profiles of the evaluated AMPs, which are crucial for their development as therapeutic agents. Hemolysis, the rupture of red blood cells, can lead to serious side effects and is a significant concern when considering the therapeutic application of peptides[49]. Our findings reveal variability in the hemolytic activity among the tested peptides, with some exhibiting a favorable safety profile while others raised concerns regarding their potential toxicity. For instance, certain standard inhibitors demonstrated low hemolytic activity. Such variations underscore the complexity of peptide interactions with host cells and highlight the importance of thorough toxicity assessments in the early stages of drug development[50]. This observation is consistent with existing literature, which indicates that the toxicity of AMPs can vary significantly based on their structure and composition. For example, several studies have reported that modifications in the amino acid sequence, charge distribution, and hydrophobicity of AMPs can dramatically influence their hemolytic activity and overall safety[51,52]. Research has shown that AMPs with a high proportion of cationic residues tend to have increased hemolytic effects due to their ability to disrupt membrane integrity[53,54]. Conversely, modifications to reduce the cationic charge can lead to decreased hemolytic activity without compromising antimicrobial efficacy, providing a dual advantage in therapeutic applications[55]. In addition, the potential for AMPs to harm host cells at elevated concentrations has been widely documented[56]. This has prompted researchers to explore strategies for optimizing peptide design to enhance therapeutic efficacy while minimizing cytotoxic effects. For instance, some studies have focused on developing peptide analogues with reduced cytotoxicity through structure-activity relationship (SAR) analyses, enabling the identification of variants with improved safety profiles[57,58]. Furthermore, the physicochemical characterization of AMPs revealed significant variations in their stability, hydrophobicity, and predicted half-life, which are crucial factors influencing their therapeutic potential. Notably, peptides such as Tachystatin, Pleurocidin, and Subtilisin A exhibited strong stability with an instability index below 40.00, indicating their potential for prolonged bioactivity and reduced degradation in physiological conditions. These findings underscore the importance of physicochemical profiling in selecting AMPs with optimal stability and safety for therapeutic applications.

In order to enhance both the binding affinity and minimize toxicity of AMPs, several strategies can be employed. Modifying the amino acid sequence, such as incorporating non-natural residues or optimizing the hydrophobicity-to-hydrophilicity ratio, could improve the specificity and binding strength of AMPs to their target receptors[59,60]. Additionally, cyclic peptides or stapled peptides have been explored to improve stability, prolong half-life, and enhance receptor binding by providing conformational rigidity that can better match receptor binding sites[61]. Another promising approach is the design of peptides with alternating cationic and hydrophobic residues. This could reduce toxicity by limiting the peptides' interactions with host cell membranes while maintaining their antimicrobial efficacy[62,63]. Furthermore, incorporating modifications that allow for selective receptor targeting, such as by adding targeting ligands or peptide sequences that promote receptor specificity, could also enhance therapeutic outcomes. By optimizing the binding affinity and safety profile of AMPs, future peptide-based therapies may become more effective and safer for clinical applications, paving the way for their use in treating infection-related cardiovascular diseases.

Clinical implications and limitations

Exploring peptide-receptor interactions has significant clinical implications, particularly in developing targeted therapies and precision medicine. Understanding the fundamental mechanisms by which peptides bind to their receptors provides crucial insights for designing novel therapeutics that target specific biological pathways more effectively. For instance, inhibiting MMPs by peptides has been shown to play a critical role in managing cardiovascular diseases by preventing the degradation of extracellular matrix components, thereby improving vascular stability and function[43,64]. Similarly, peptides that target ACE2 could potentially modulate cardiovascular disease outcomes, offering new avenues for treatment[41]. These findings underscore the importance of peptide-receptor interactions in crafting targeted therapeutic interventions. However, several limitations associated with peptide-based therapies must be addressed. One primary challenge is the stability of peptides in physiological conditions, which often impacts their efficacy. Peptides are susceptible to rapid degradation by proteolytic enzymes, reducing their therapeutic potential and necessitating the development of strategies to enhance their stability[65,66]. For instance, many peptides can be hydrolyzed by enzymes like trypsin and chymotrypsin, which

are abundant in the digestive system[67]. This enzymatic action can result in the loss of the peptides' bioactive properties before they reach their intended target sites. Moreover, the rapid turnover and clearance of peptides from the systemic circulation can limit their effective concentration at the site of action, necessitating frequent dosing to achieve desired therapeutic outcomes[68]. Therefore, it is crucial to develop strategies to enhance peptide stability and resistance to enzymatic degradation. Such strategies may include chemical modifications, such as incorporating non-proteogenic amino acids or using cyclization to create more stable structures[69,70]. Additionally, the specificity of peptide-receptor interactions is crucial for minimizing off-target effects and maximizing therapeutic outcomes[71]. When comparing AMPs to standard inhibitors like DX600, our findings indicate that AMPs such as Tachystatin and Pleurocidin demonstrate superior binding affinities and stability, which could offer significant therapeutic advantages. For instance, Tachystatin's binding energy of −10.7 kcal/mol with ACE2 surpasses that of DX600, which has a binding energy of −8.6kcal/mol. This stronger binding affinity suggests that Tachystatin may provide more potent inhibition of ACE2, potentially resulting in a longer duration of action and a reduced need for frequent dosing. Moreover, AMPs exhibit stable interactions with their target proteins, which could enhance their effectiveness in vivo by maintaining therapeutic concentrations over longer periods, especially under the dynamic conditions of the human body. These properties are crucial for developing effective peptide-based therapeutics, as they would likely improve the treatment outcomes while minimizing the potential for resistance or off-target effects. While advances in computational modeling and simulations have improved our understanding of these interactions, translating these findings into clinical applications remains challenging[72]. Another limitation is the potential for adverse immune responses to peptide-based therapies. Peptides can sometimes trigger immune reactions, leading to reduced patient efficacy or adverse effects[73,74]. Furthermore, the cost and complexity of developing and producing peptide-based drugs can be significant, potentially limiting their accessibility and widespread use[75,76]. Therefore, while peptide-based therapeutics offer promising prospects, ongoing research and development are needed to address these limitations and optimize their clinical application.

Future works

In future studies, we plan to include a broader range of AMPs with diverse structural characteristics, mechanisms of action, and target affinities. By expanding the selection of AMPs, we aim to enhance the robustness of our findings and provide a more comprehensive analysis of their potential therapeutic applications in combating infection-related cardiovascular diseases. Additionally, incorporating AMPs from various sources, such as plants, animals, and microorganisms, could offer new insights into developing novel strategies for treating infections while minimizing the risks of resistance and cytotoxicity. This approach will allow for a more thorough evaluation of AMPs as viable therapeutic agents and their potential to improve cardiovascular health. Furthermore, future studies will involve in vitro assays to assess the antimicrobial efficacy, hemolytic activity, and cytotoxicity of selected AMPs, followed by in vivo animal models to evaluate their therapeutic potential and safety profiles. We also plan to incorporate well-known CVD-modulating peptides or drugs as controls to benchmark the efficacy of the selected AMPs. This comparative approach will provide a more nuanced understanding of the relative effectiveness of the AMPs, ensuring that our findings are robust and aligned with established therapeutic strategies. These combined efforts will provide deeper insights into the pharmacological and clinical applicability of AMPs in infection-related cardiovascular disease treatments.

Conclusions

In conclusion, the molecular docking and dynamics simulations provide compelling insights into the interactions of AMPs with receptors implicated in infection-related CVDs. Our simulations indicated that Tachystatin, Thermolysin, Pleurocidin, and Subtilisin A exhibited favorable binding affinities and stability with key receptors such as ACE2, CRP, MMP9, NLRP3, and TLR4 compared to the standard inhibitor DX600. Tachystatin demonstrated consistent and strong binding with multiple receptors, including ACE2 and MMP9, with favorable HADDOCK scores and binding energies. Thermolysin and Pleurocidin also showed potential, exhibiting significant interaction profiles and stability across different receptor complexes. Subtilisin A, while showing robust performance with CRP and NLRP3, demonstrated impressive binding characteristics with TLR4. The detailed analysis of energy components, intermolecular contacts, and hydrogen bonds further supports the potential for these AMPs to disrupt receptor-mediated infection pathways. While the results from this in silico study highlight the promise of these AMPs, it is crucial to note that further experimental validation, including in vitro and preclinical studies, is needed to establish their therapeutic efficacy. Future research should aim to translate these findings into practical applications for preventing and treating CVDs associated with infection and inflammation.

Materials and methods

Selection and preparation of the receptors associated with infection-related CVDs

In this study, five key receptors associated with infection-related CVDs were selected for analysis: Angiotensin-Converting Enzyme 2 (ACE2), C-reactive protein (CRP), Matrix Metalloproteinase-9 (MMP9), NLRP3 Inflammasome, and Toll-Like Receptor-4 (TLR4) (Table 8). The selection of these receptors was based on their critical involvement in both microbial infection processes and the progression of cardiovascular diseases. ACE2 plays a significant role in regulating blood pressure and is implicated in cardiovascular complications, particularly in the context of viral infections such as SARS-CoV-2[77]. CRP, a well-established inflammatory marker, is involved in the inflammatory response associated with cardiovascular diseases[78]. MMP9 is crucial in extracellular matrix remodeling and atherosclerotic plaque instability[79]. NLRP3 is a key component of the inflammasome that contributes to the inflammatory processes in CVDs[80], while TLR4 plays a pivotal role in

recognizing pathogen-associated molecular patterns and triggering immune responses linked to atherosclerosis and other cardiovascular conditions[81].

These receptors were selected due to their well-characterized functions in the pathogenesis of infection-related CVDs and the availability of high-resolution 3D structures in the Protein Data Bank (PDB), which ensured that precise molecular docking and dynamics simulations could be conducted. The preparation process involved retrieving the structural data from the PDB, optimizing the protein structures, and refining them using Swiss-PdbViewer[82]v4.1 to correct potential issues and enhance model accuracy. This refinement process included adjusting side-chain conformations, adding missing residues, and validating structural quality, ensuring the receptors were suitable for accurate interaction modeling. Additionally, their active sites were defined using CASTp 3.0[83], facilitating detailed docking studies with the selected antimicrobial peptides.

Selection and preparation of antimicrobial peptides (AMPs)

Specific criteria were employed to guide the selection of AMPs for this study, ensuring the relevance and reliability of the molecular docking and dynamics simulations. Only peptides with available 3D structures in the PDB were considered, guaranteeing the availability of accurate structural data necessary for effective modeling and simulation. The peptides chosen were classified under the SCOP (Structural Classification of Proteins) as "peptides." The resolution of the structural data was restricted to 0.5–2.5 Å, as high-resolution structures are preferred for their detailed and accurate depiction of peptide conformation, which is crucial for precise docking simulations. The binding regions of the AMPs were analyzed using CASTp 3.0[83]. The complete dataset, including type, PDB ID, sequence, and active residues of the selected AMPs, is provided in Supplementary Data 3.

Based on these criteria, a set of 30 AMPs was chosen (Table 9), including Exendin-4, an AMP with similarities to GLP-1, and has been investigated for its potential to influence ACE2 activity[120]. CRP is a marker of inflammation often elevated in cardiovascular diseases[78]. Lactoferrin, an iron-binding glycoprotein known for its antimicrobial properties, has been shown to affect CRP levels[121], thus, Lactoferrin potentially influences cardiovascular outcomes and highlights its role in controlling inflammation in cardiovascular diseases. Cathelicidin, another well-studied AMP, has been shown to modulate the NLRP3 inflammasome, a critical component of the inflammatory response linked to cardiovascular diseases[122]. These examples illustrate how AMPs interact with key receptors involved in cardiovascular diseases, offering valuable insights into their potential therapeutic applications for modulating receptor activity and managing disease progression.

Molecular docking simulations

In this phase, molecular docking simulations were meticulously performed to investigate the interactions between a selected set of AMPs and specific receptors implicated in cardiovascular diseases. These receptors are critical targets in cardiovascular diseases and infections, influencing disease progression and inflammatory responses. The molecular docking simulations aimed to investigate the interactions between the selected AMPs and CVD-related receptors associated with infection and inflammation pathways. Key interaction parameters were analyzed to understand better how AMPs bind to these target receptors. The docking results included an evaluation of the HADDOCK score, free binding energy (kcal/mol), van der Waals energy, electrostatic energy, and desolvation energy for various AMP-receptor combinations. The simulations were executed using the stand-alone version of HADDOCK (High Ambiguity Driven protein-protein DOCKing)[123], a robust and versatile docking software that enables detailed exploration of binding modes and energetic interactions between complex biomolecules. HADDOCK is well-regarded for incorporating experimental data into the docking process, allowing for a more accurate prediction of the possible binding conformations between AMPs and target receptors. The DX600 peptide (sequence: GDYSHCSPLRYYPWWKCTYPDPEGGG) was used as a reference standard due to its known interaction with CVD-related receptors like ACE2 (IC_{50}: 10.1 μM) and therapeutic implications in cardiovascular conditions[89]. The 3D structure of peptide 35,409 was generated using AlphaFold[124], providing a precise model for further analysis. DX600 peptide was utilized as a benchmark to evaluate the efficacy of other AMPs in binding to the target receptors. Using this standard peptide allowed for a comparative analysis of the binding efficiency and inhibitory potential of other AMPs. The insights gained from these simulations are intended to guide the selection of AMPs with the highest potential for therapeutic applications. To further refine and validate the docking results, PRODIGY (PROtein binDIng enerGY prediction)[125]was employed to predict the binding affinity of the AMP-adhesion protein complexes. PRODIGY is an advanced computational tool that leverages state-of-the-art algorithms to estimate the binding affinity between interacting proteins and ligands based on structural data[126]. This prediction of binding free energy is critical for ranking the AMP candidates, as it provides a quantitative measure of how strongly an AMP binds to a target receptor. By identifying the AMPs with the most favorable binding affinities, PRODIGY helps narrow down the candidates most likely to impact cardiovascular disease receptors effectively. All molecular docking simulations were conducted on a high-performance computing workstation with an Intel® Core™ i7-12650 H processor, an NVIDIA™ RTX 4060 graphics card with 8 GB VRAM, and 16 GB of DDR5 RAM.

Molecular dynamics (MD) simulations

Molecular dynamics (MD) simulations were employed to investigate AMP-receptor complexes' dynamic behavior and stability, specifically focusing on the interactions between AMPs and receptors involved in infection-related CVDs. The simulations were performed using GROMACS 2022.5[127], a well-established software package known for its high computational efficiency and reliability in simulating biomolecular systems. The OPLS-AA/L (Optimized Potentials for Liquid Simulations) force field was selected due to its proven accuracy in modeling protein-ligand interactions[128], especially in studies involving peptides and proteins, ensuring reliable prediction of molecular interactions within the complexes. Simulation systems were constructed using default cubic box parameters to ensure sufficient space for the AMP-receptor complexes, allowing them to move freely during

Antimicrobial peptide	PDB ID	Size (kDa)	Binding regions (Position of residues)	Ref
DX600 (standard inhibitor)	N/A	3.04	18, 19	89
Aurein	1VM5	1.48	1, 2, 5	90
Beta-defensin 2	1FD4	7.04	6, 7, 9, 10, 11, 12	91
Bombinin	2AP7	1.98	1, 3, 4, 6, 7	92
Cathelicidin	2K6O	4.49	1, 4, 5, 8	93
Cecropin	1D9J	2.23	7, 9, 10, 11, 12	94
Chim2	8EB1	2.94	10, 11, 14, 15	95
Dermcidin	2NDK	4.82	18, 19, 22, 25, 26, 29	96
Esculentin	5XDJ	4.80	2, 3, 6	97
Exendin-4	3C59	2.99	26, 27, 28, 29, 32, 33	98
Hepcidin	3H0T	2.48	13, 14, 16, 18, 19, 20, 21, 22	99
Hs05	6VLA	2.06	5, 8, 9	100
Indolicidin	1HR1	1.83	9, 10, 11, 12, 13	101
Lactoferrin	1LFC	3.13	1, 23, 25	102
Lavracin	2N8D	2.25	1, 3, 4, 6	103
Magainin	2MAG	2.47	1, 2, 6, 9, 17, 21	104
Melittin	2MLT	7.59	13, 16, 17, 20	105
Microcin J25	4CU4	2.13	9, 10, 19, 20, 21	106
Nisin	1WCO	5.94	9, 12, 17, 19, 20, 21	107
Pardaxin	2KNS	3.32	2, 3, 5, 6, 9, 15, 22, 23, 26, 27, 29, 30, 33	108
Piscidin	6PEZ	2.49	3, 4, 7	109
Pleurocidin	2LS9	2.71	10, 13, 14, 17, 20, 23, 24	110
Polyphemusin I	1RKK	2.46	7, 9, 12, 14	111
Protegrin-1	1PG1	2.16	5, 6, 7, 14, 15, 16	112
PvHCt	2N1C	2.75	14, 15, 16, 17, 18, 19, 20, 22, 23	113
Subtilisin A	1PXQ	3.43	1, 4, 5, 7, 9, 10, 24, 25, 29, 30, 33	114
Tachyplesin-1	2RTV	2.27	1, 2, 3, 16, 17	115
Tachystatin	1CIX	7.51	5, 11, 12, 15, 18, 22, 23, 29	116
Temporin-L	6GS5	1.64	4, 7	117
Thanatin	8TFV	2.44	11, 13, 16, 17, 18	118
Thermolysin	6FHP	6.30	258, 263, 267, 305, 306, 309, 310	119

Table 9. Selected antimicrobial peptides (AMPs) based on the employed criterion. It includes their respective PDB ids, molecular sizes (kDa), and binding regions, which are essential for assessing their binding capabilities and therapeutic relevance in infection-related CVDs.

the simulation. Water molecules were added to model the solvent environment using the Single Point Charge Extended (SPCE) model[129], a widely accepted water model in MD simulations. This model ensures that the water molecules interact appropriately with the system. Counterions (typically Na^+ and Cl^-) were added to neutralize the system, ensuring the overall charge balance required for the accuracy of the simulation. Energy minimization was performed using the steepest-descent method for system preparation to remove any steric clashes or unfavorable interactions that could arise from the initial configuration. This step helps relax the system and bring it into a more stable state before proceeding with equilibration and production runs. The equilibration process was conducted in two distinct stages. NVT ensemble (constant number of particles, volume, and temperature) was used in the first stage to stabilize the system's temperature at 300 K. This step ensures that the system reaches thermal equilibrium, with the temperature of the complex held constant throughout the equilibration phase. NPT ensemble (constant number of particles, pressure, and temperature) was used in the second stage to stabilize the system further and maintain a constant pressure of 1 bar during the simulation. This allows the system to adapt to physiological conditions, ensuring the accuracy of the dynamics, especially for large biomolecular systems like AMP-receptor complexes[37,130]. After successful equilibration, production MD simulations were carried out for a total duration of 100 nanoseconds. This extended simulation time allowed for analyzing the AMP-receptor complexes' long-term stability and dynamic behavior. Throughout the production simulation, parameters like Root Mean Square Deviation (RMSD), Root Mean Square Fluctuation (RMSF), Radius of Gyration (RoG), potential energy, and hydrogen bonding interactions were continuously monitored and analyzed. Molecular visualization software, including PyMOL[131] and UCSF Chimera[132], was used to visualize critical residues and intermolecular interactions within the simulated complexes. This analysis provided valuable insights into the binding mechanisms and stability of the AMPs with the cardiovascular disease receptors. In addition to the default simulation parameters, temperature and pressure coupling were carefully managed

using the Berendsen thermostat and Berendsen barostat, respectively, to ensure smooth equilibration and stable production runs. The long-time scale of the MD simulations (100 ns) enabled the observation of rare conformational changes and binding events that may not be captured in shorter simulations, providing a more comprehensive understanding of AMP-receptor dynamics.

Molecular mechanics/poisson–boltzmann surface area (MM/PBSA) calculations
The Molecular Mechanics/Poisson-Boltzmann Surface Area (MM/PBSA) method evaluated the peptide-receptor interactions involving AMPs and receptors implicated in infection-related CVDs. This method utilizes MD simulation data to calculate the binding free energy of the AMP-receptor complexes, providing insights into the strength and stability of these interactions. The MD simulations generated a variety of receptor conformations, and representative snapshots from these simulations were selected for detailed analysis[133]. Comprehensive energy computations were performed for each snapshot, including gas-phase energy calculations, solvation energy estimation using a continuum solvent model, and entropy calculations. These components were integrated to determine the overall binding free energy of the AMP-receptor complex[134,135]. The calculations used the *gmx_MMPBSA*module available within the GROMACS simulation package[136,137]. It is well-regarded for its precision and efficiency in calculating binding free energies for biomolecular complexes. The MM/PBSA method is precious for predicting binding affinities, as it accounts for the energetic and solvation contributions to the binding process[138]. The binding free energy (ΔG_binding) was computed using the following equation:

$$\Delta G_binding = \Delta G_complex - \Delta G_peptide - \Delta G_protein$$

Where:
ΔG_binding: the binding free energy associated with forming the peptide-protein complex.
ΔG_complex: the free energy of the fully solvated peptide-protein complex.
ΔG_peptide: the free energy of peptide in its solvated state when unbound.
ΔG_protein: the free energy of protein in its solvated state when unbound.
By calculating the difference between the free energy of the complex and the combined free energies of the unbound AMP and receptor, this method provided insights into the energetic changes that occur upon complex formation, elucidating the interaction's strength and stability.

Haemolytic activity prediction of antimicrobial peptides (AMPs)
The haemolytic activity of selected AMPs was evaluated using the Hemolytic Activity Prediction for Peptides and Proteins (HAPPENN) tool. HAPPENN is a novel computational tool designed specifically for predicting the hemolytic potential of therapeutic peptides by employing advanced neural network algorithms[139]. The amino acid sequences of the selected AMPs were input into the HAPPENN platform to conduct the haemolytic activity assessment. This tool utilizes a dataset of known peptides with established haemolytic activity to train its neural network. The training process involves analyzing the structural and compositional features of the peptides, such as hydrophobicity, charge distribution, and amino acid sequences, which are critical in determining their interaction with erythrocyte membranes. Once the input sequences were processed, HAPPENN generated predictions regarding the haemolytic potential of each peptide. The output includes a quantitative score that reflects the likelihood of a given AMP to induce hemolysis in red blood cells, allowing for a comparative assessment of the AMPs' safety profiles.

Physicochemical characterization of antimicrobial peptides (AMPs)
The physicochemical properties of AMPs were analyzed using the ProtParam tool[140], which computes various parameters from a given protein sequence. The sequences of AMPs, including DX600 (a standard inhibitor), were input into ProtParam to determine theoretical isoelectric points (pI), extinction coefficients (M^{-1} cm^{-1} at 280 nm), estimated half-life in mammalian reticulocytes (in vitro), instability index, aliphatic index, and grand average of hydropathicity (GRAVY). The extinction coefficient was calculated based on the presence of tyrosine, tryptophan, and cystine residues, while the estimated half-life was predicted using the "N-end rule." The instability index classified peptides as stable (≤ 40.00) or unstable (> 40.00), the aliphatic index indicated thermostability based on aliphatic side chain volume, and GRAVY assessed hydrophobicity or hydrophilicity. These parameters provide insights into AMP stability, solubility, and potential biological activity.

Data availability
Data is provided within the manuscript or supplementary information files.

Received: 2 November 2024; Accepted: 10 March 2025
Published online: 14 March 2025

References
1. Rademacher, J. et al. Association of respiratory infections and the impact of vaccinations on cardiovascular diseases. *Eur. J. Prev. Cardiol.* **31**, 877–888. https://doi.org/10.1093/eurjpc/zwae016 (2024).
2. Stotts, C., Corrales-Medina, V. F. & Rayner, K. J. Pneumonia-Induced inflammation, resolution and cardiovascular disease: causes, consequences and clinical opportunities. *Circul. Res.* **132**, 751–774. https://doi.org/10.1161/CIRCRESAHA.122.321636 (2023).
3. Shayista, H. et al. Mechanistic overview of gut microbiota and mucosal pathogens with respect to cardiovascular diseases. *Microbe* **5**, 100160. https://doi.org/10.1016/j.microb.2024.100160 (2024).
4. Chen, L. et al. Inflammatory responses and inflammation-associated diseases in organs. *Oncotarget* **9**, 7204–7218. https://doi.org/10.18632/oncotarget.23208 (2018).

5. Yang, T. H. et al. A review on the pathogenesis of cardiovascular disease of flaviviridea viruses infection. *Viruses* **16**, 365 (2024).
6. Liu, C. & Waters, D. D. Chlamydia pneumoniae and atherosclerosis: from Koch postulates to clinical trials. *Prog Cardiovasc. Dis.* **47**, 230–239. https://doi.org/10.1016/j.pcad.2005.01.001 (2005).
7. Jung, S. H. & Lee, K. T. Atherosclerosis by virus Infection-A short review. *Biomedicines* **10** https://doi.org/10.3390/biomedicines10102634 (2022).
8. Wolf, D. & Ley, K. Immunity and inflammation in atherosclerosis. *Circ. Res.* **124**, 315–327. https://doi.org/10.1161/circresaha.118.313591 (2019).
9. Laera, N. et al. Impact of immunity on coronary artery disease: an updated pathogenic interplay and potential therapeutic strategies. *Life (Basel)*. **13** https://doi.org/10.3390/life13112128 (2023).
10. Jaén, R. I. et al. Innate immune receptors, key actors in cardiovascular diseases. *JACC: Basic. Translational Sci.* **5**, 735–749. https://doi.org/10.1016/j.jacbts.2020.03.015 (2020).
11. Kircheis, R. & Planz, O. The role of Toll-like receptors (TLRs) and their related signaling pathways in viral infection and inflammation. *Int. J. Mol. Sci.* **24** https://doi.org/10.3390/ijms24076701 (2023).
12. Goulopoulou, S., McCarthy, C. G. & Webb, R. C. Toll-like receptors in the vascular system: sensing the dangers within. *Pharmacol. Rev.* **68**, 142–167. https://doi.org/10.1124/pr.114.010090 (2016).
13. Tanase, D. M. et al. Portrayal of NLRP3 inflammasome in atherosclerosis: current knowledge and therapeutic targets. *Int. J. Mol. Sci.* **24** https://doi.org/10.3390/ijms24098162 (2023).
14. Karasawa, T. & Takahashi, M. Role of NLRP3 inflammasomes in atherosclerosis. *J. Atheroscler Thromb.* **24**, 443–451. https://doi.org/10.5551/jat.RV17001 (2017).
15. Bourgonje, A. R. et al. Angiotensin-converting enzyme 2 (ACE2), SARS-CoV-2 and the pathophysiology of coronavirus disease 2019 (COVID-19). *J. Pathol.* **251**, 228–248. https://doi.org/10.1002/path.5471 (2020).
16. Liu, L. P., Zhang, X. L. & Li, J. New perspectives on angiotensin-converting enzyme 2 and its related diseases. *World J. Diabetes.* **12**, 839–854. https://doi.org/10.4239/wjd.v12.i6.839 (2021).
17. Cao, Q. et al. Impact of cardiovascular diseases on COVID-19: A systematic review. *Med. Sci. Monit.* **27**, e930032. https://doi.org/10.12659/msm.930032 (2021).
18. Olejarz, W., Łacheta, D. & Kubiak-Tomaszewska, G. Matrix metalloproteinases as biomarkers of atherosclerotic plaque instability. *Int. J. Mol. Sci.* **21** https://doi.org/10.3390/ijms21113946 (2020).
19. Liu, P., Sun, M. & Sader, S. Matrix metalloproteinases in cardiovascular disease. *Can. J. Cardiol.* **22 Suppl B**, 25b–30b. https://doi.org/10.1016/s0828-282x(06)70983-7 (2006).
20. Porritt, R. A. & Crother, T. R. Chlamydia pneumoniae infection and inflammatory diseases. *Immunopathol. Dis. Th.* **7**, 237–254. https://doi.org/10.1615/ForumImmunDisTher.2017020161 (2016).
21. Muhlestein, J. B. et al. Infection with Chlamydia pneumoniae accelerates the development of atherosclerosis and treatment with Azithromycin prevents it in a rabbit model. *Circulation* **97**, 633–636. https://doi.org/10.1161/01.CIR.97.7.633 (1998).
22. Llor, C. & Bjerrum, L. Antimicrobial resistance: risk associated with antibiotic overuse and initiatives to reduce the problem. *Ther. Adv. Drug Saf.* **5**, 229–241. https://doi.org/10.1177/2042098614554919 (2014).
23. Muteeb, G., Rehman, M. T., Shahwan, M. & Aatif, M. Origin of antibiotics and antibiotic resistance, and their impacts on drug development: A narrative review. *Pharmaceuticals (Basel)*. 16. https://doi.org/10.3390/ph16111615 (2023).
24. Ahmed, S. K. et al. Antimicrobial resistance: impacts, challenges, and future prospects. *J. Med. Surg. Public. Health.* **2**, 100081. https://doi.org/10.1016/j.glmedi.2024.100081 (2024).
25. Heianza, Y. et al. Duration and life-stage of antibiotic use and risk of cardiovascular events in women. *Eur. Heart J.* **40**, 3838–3845. https://doi.org/10.1093/eurheartj/ehz231 (2019).
26. Luong, H. X., Thanh, T. T. & Tran, T. H. Antimicrobial peptides - Advances in development of therapeutic applications. *Life Sci.* **260**, 118407. https://doi.org/10.1016/j.lfs.2020.118407 (2020).
27. Xuan, J. et al. Antimicrobial peptides for combating drug-resistant bacterial infections. *Drug Resist. Updates.* **68**, 100954. https://doi.org/10.1016/j.drup.2023.100954 (2023).
28. Benfield, A. H. & Henriques, S. T. Mode-of-Action of antimicrobial peptides: membrane disruption vs. Intracellular mechanisms. *Front. Med. Technol.* **2**, 610997. https://doi.org/10.3389/fmedt.2020.610997 (2020).
29. Gong, H. et al. How do antimicrobial peptides disrupt the lipopolysaccharide membrane leaflet of Gram-negative bacteria? *J. Colloid Interface Sci.* **637**, 182–192. https://doi.org/10.1016/j.jcis.2023.01.051 (2023).
30. Zhang, Q. Y. et al. Antimicrobial peptides: mechanism of action, activity and clinical potential. *Military Med. Res.* **8** https://doi.org/10.1186/s40779-021-00343-2 (2021).
31. Singh, R. & Purohit, R. Computational analysis of protein-ligand interaction by targeting a cell cycle restrainer. *Comput. Methods Programs Biomed.* **231**, 107367. https://doi.org/10.1016/j.cmpb.2023.107367 (2023).
32. Singh, R., Bhardwaj, V. K. & Purohit, R. Inhibition of nonstructural protein 15 of SARS-CoV-2 by golden Spice: A computational insight. *Cell. Biochem. Funct.* **40**, 926–934. https://doi.org/10.1002/cbf.3753 (2022).
33. Kalsi, N., Gopalakrishnan, C., Rajendran, V. & Purohit, R. Biophysical aspect of phosphatidylinositol 3-kinase and role of oncogenic mutants (E542K & E545K). *J. Biomol. Struct. Dyn.* **34**, 2711–2721. https://doi.org/10.1080/07391102.2015.1127774 (2016).
34. Bhardwaj, V., Singh, R., Singh, P., Purohit, R. & Kumar, S. Elimination of bitter-off taste of stevioside through structure modification and computational interventions. *J. Theor. Biol.* **486**, 110094. https://doi.org/10.1016/j.jtbi.2019.110094 (2020).
35. Singh, R., Bhardwaj, V. K., Sharma, J., Das, P. & Purohit, R. Identification of selective cyclin-dependent kinase 2 inhibitor from the library of pyrrolone-fused benzosuberene compounds: an in Silico exploration. *J. Biomol. Struct. Dyn.* **40**, 7693–7701. https://doi.org/10.1080/07391102.2021.1900918 (2022).
36. Bhardwaj, V. K. & Purohit, R. A comparative study on inclusion complex formation between Formononetin and β-cyclodextrin derivatives through multiscale classical and umbrella sampling simulations. *Carbohydr. Polym.* **310**, 120729. https://doi.org/10.1016/j.carbpol.2023.120729 (2023).
37. Dermawan, D., Sumirtanurdin, R. & Dewantisari, D. Simulasi Dinamika Molekular reseptor Estrogen Alfa Dengan andrografolid Sebagai anti Kanker Payudara. *Indones J. Pharm. Sci. Technol.* **6**, 65–76 (2019).
38. Nnyigide, O. S., Lee, S. G. & Hyun, K. Silico characterization of the binding modes of surfactants with bovine serum albumin. *Sci. Rep.* **9**, 10643. https://doi.org/10.1038/s41598-019-47135-2 (2019).
39. Zasloff, M. Antimicrobial peptides of multicellular organisms. *Nature* **415**, 389–395. https://doi.org/10.1038/415389a (2002).
40. Ganz, T. Defensins: antimicrobial peptides of innate immunity. *Nat. Rev. Immunol.* **3**, 710–720. https://doi.org/10.1038/nri1180 (2003).
41. Festa, M. et al. Cardiovascular active peptides of marine origin with ACE inhibitory activities: potential role as Anti-Hypertensive drugs and in prevention of SARS-CoV-2 infection. *Int. J. Mol. Sci.* **21** https://doi.org/10.3390/ijms21218364 (2020).
42. Lee, R. T. Matrix metalloproteinase Inhibition and the prevention of heart failure. *Trends Cardiovasc. Med.* **11**, 202–205. https://doi.org/10.1016/s1050-1738(01)00113-x (2001).
43. Ndinguri, M. W., Bhowmick, M., Tokmina-Roszyk, D., Robichaud, T. K. & Fields, G. B. Peptide-based selective inhibitors of matrix metalloproteinase-mediated activities. *Molecules* **17**, 14230–14248. https://doi.org/10.3390/molecules171214230 (2012).
44. Al Musaimi, O., Lombardi, L., Williams, D. R. & Albericio, F. Strategies for improving peptide stability and delivery. *Pharmaceuticals (Basel)*. **15** https://doi.org/10.3390/ph15101283 (2022).

45. Hossain, M. S. et al. Therapeutic potential of antiviral peptides against the NS2B/NS3 protease of Zika virus. *ACS Omega*. **8**, 35207–35218. https://doi.org/10.1021/acsomega.3c04903 (2023).
46. Dermawan, D., Bahtiar, R. & Sofian, F. F. Implementation of green supply chain management (GSCM) in the pharmaceutical industry in Indonesia: feasibility analysis and case studies. *J. Ilm Farm.* **15**, 23–29 (2019).
47. Kastritis, P. L. & Bonvin, A. M. On the binding affinity of macromolecular interactions: daring to ask why proteins interact. *J. R Soc. Interface*. **10**, 20120835. https://doi.org/10.1098/rsif.2012.0835 (2013).
48. Lin, D. et al. Improved functionality and safety of peptides by the formation of peptide-polyphenol complexes. *Trends Food Sci. Technol.* **141**, 104193. https://doi.org/10.1016/j.tifs.2023.104193 (2023).
49. Robles-Loaiza, A. A. et al. Traditional and computational screening of Non-Toxic peptides and approaches to improving selectivity. *Pharmaceuticals (Basel)*. **15** https://doi.org/10.3390/ph15030323 (2022).
50. Amorim, A. M. B. et al. Advancing drug safety in drug development: bridging computational predictions for enhanced toxicity prediction. *Chem. Res. Toxicol.* **37**, 827–849. https://doi.org/10.1021/acs.chemrestox.3c00352 (2024).
51. Aoki, W. & Ueda, M. Characterization of antimicrobial peptides toward the development of novel antibiotics. *Pharmaceuticals (Basel)*. **6**, 1055–1081. https://doi.org/10.3390/ph6081055 (2013).
52. Schmidtchen, A., Pasupuleti, M. & Malmsten, M. Effect of hydrophobic modifications in antimicrobial peptides. *Adv. Colloid Interface Sci.* **205** https://doi.org/10.1016/j.cis.2013.06.009 (2013).
53. Zhu, X. et al. Characterization of antimicrobial activity and mechanisms of low amphipathic peptides with different α-helical propensity. *Acta Biomater.* **18**, 155–167. https://doi.org/10.1016/j.actbio.2015.02.023 (2015).
54. Zhang, Q. Y. et al. Antimicrobial peptides: mechanism of action, activity and clinical potential. *Mil Med. Res.* **8**, 48. https://doi.org/10.1186/s40779-021-00343-2 (2021).
55. Rotem, S., Radzishevsky, I. & Mor, A. Physicochemical properties that enhance discriminative antibacterial activity of short dermaseptin derivatives. *Antimicrob. Agents Chemother.* **50**, 2666–2672. https://doi.org/10.1128/aac.00030-06 (2006).
56. Zainal Baharin, N. H. et al. The characteristics and roles of antimicrobial peptides as potential treatment for antibiotic-resistant pathogens: a review. *PeerJ* **9**, e12193. https://doi.org/10.7717/peerj.12193 (2021).
57. Amatuni, A., Shuster, A., Abegg, D., Adibekian, A. & Renata, H. Comprehensive Structure-Activity relationship studies of Cepafungin enabled by biocatalytic C-H oxidations. *ACS Cent. Sci.* **9**, 239–251. https://doi.org/10.1021/acscentsci.2c01219 (2023).
58. Guha, R. On exploring Structure–Activity relationships. *Methods in molecular biology. (Clifton N J)*. **993**, 81–94. https://doi.org/10.1007/978-1-62703-342-8_6 (2013).
59. Mwangi, J., Kamau, P. M., Thuku, R. C. & Lai, R. Design methods for antimicrobial peptides with improved performance. *Zool. Res.* **44**, 1095–1114. https://doi.org/10.24272/j.issn.2095-8137.2023.246 (2023).
60. Gagat, P., Ostrówka, M., Duda-Madej, A. & Mackiewicz, P. Enhancing antimicrobial peptide activity through modifications of charge, hydrophobicity, and structure. *Int. J. Mol. Sci.* **25**, 10821 (2024).
61. Li, Y. et al. Therapeutic stapled peptides: efficacy and molecular targets. *Pharmacol. Res.* **203**, 107137. https://doi.org/10.1016/j.phrs.2024.107137 (2024).
62. Gagat, P., Ostrówka, M., Duda-Madej, A. & Mackiewicz, P. Enhancing antimicrobial peptide activity through modifications of charge, hydrophobicity, and structure. *Int. J. Mol. Sci.* **25** https://doi.org/10.3390/ijms251910821 (2024).
63. Liang, Q. et al. Development strategies and application of antimicrobial peptides as future alternatives to in-feed antibiotics. *Sci. Total Environ.* **927**, 172150. https://doi.org/10.1016/j.scitotenv.2024.172150 (2024).
64. Fan, Z. et al. Sustained release of a Peptide-Based matrix Metalloproteinase-2 inhibitor to attenuate adverse cardiac remodeling and improve cardiac function following myocardial infarction. *Biomacromolecules* **18**, 2820–2829. https://doi.org/10.1021/acs.biomac.7b00760 (2017).
65. Evans, B. J., King, A. T., Katsifis, A., Matesic, L. & Jamie, J. F. Methods to enhance the metabolic stability of Peptide-Based PET radiopharmaceuticals. *Molecules* **25** https://doi.org/10.3390/molecules25102314 (2020).
66. Böttger, R., Hoffmann, R. & Knappe, D. Differential stability of therapeutic peptides with different proteolytic cleavage sites in blood, plasma and serum. *PLoS One*. **12**, e0178943. https://doi.org/10.1371/journal.pone.0178943 (2017).
67. Ryan, J. T., Ross, R. P., Bolton, D., Fitzgerald, G. F. & Stanton, C. Bioactive peptides from muscle sources: meat and fish. *Nutrients* **3**, 765–791. https://doi.org/10.3390/nu3090765 (2011).
68. Musliha, A., Dermawan, D., Rahayu, P. & Tjandrawinata, R. R. Unraveling modulation effects on albumin synthesis and inflammation by Striatin, a bioactive protein fraction isolated from < em > Channa striata: *In silico proteomics and < em > in vitro approaches. Heliyon 10*. https://doi.org/10.1016/j.heliyon.2024.e38386 *(2024)*.
69. Han, Y., Zhang, M., Lai, R. & Zhang, Z. Chemical modifications to increase the therapeutic potential of antimicrobial peptides. *Peptides* **146**, 170666. https://doi.org/10.1016/j.peptides.2021.170666 (2021).
70. Ding, Y. et al. Impact of non-proteinogenic amino acids in the discovery and development of peptide therapeutics. *Amino Acids*. **52**, 1207–1226. https://doi.org/10.1007/s00726-020-02890-9 (2020).
71. Cavallaro, P. A. et al. Peptides targeting HER2-Positive breast Cancer cells and applications in tumor imaging and delivery of chemotherapeutics. *Nanomaterials (Basel)*. **13** https://doi.org/10.3390/nano13172476 (2023).
72. Ahn, W. Y. & Busemeyer, J. R. Challenges and promises for translating computational tools into clinical practice. *Curr. Opin. Behav. Sci.* **11**, 1–7. https://doi.org/10.1016/j.cobeha.2016.02.001 (2016).
73. Mahadik, R., Kiptoo, P., Tolbert, T. & Siahaan, T. J. Immune modulation by antigenic peptides and antigenic peptide conjugates for treatment of multiple sclerosis. *Med. Res. Arch.* **10** https://doi.org/10.18103/mra.v10i5.2804 (2022).
74. Jawa, V. et al. T-Cell dependent immunogenicity of protein therapeutics Pre-clinical assessment and Mitigation-Updated consensus and review 2020. *Front. Immunol.* **11**, 1301. https://doi.org/10.3389/fimmu.2020.01301 (2020).
75. Rossino, G. et al. Peptides as therapeutic agents: challenges and opportunities in the green transition era. *Molecules* **28** https://doi.org/10.3390/molecules28207165 (2023).
76. Wang, L. et al. Therapeutic peptides: current applications and future directions. *Signal. Transduct. Target. Therapy*. **7**, 48. https://doi.org/10.1038/s41392-022-00904-4 (2022).
77. Saponaro, F. et al. ACE2 in the era of SARS-CoV-2: controversies and novel perspectives. *Front. Mol. Biosci.* **7**, 588618. https://doi.org/10.3389/fmolb.2020.588618 (2020).
78. Amezcua-Castillo, E. et al. C-Reactive protein: the quintessential marker of systemic inflammation in coronary artery Disease-Advancing toward precision medicine. *Biomedicines* **11** https://doi.org/10.3390/biomedicines11092444 (2023).
79. Li, T. et al. The role of matrix Metalloproteinase-9 in atherosclerotic plaque instability. *Mediators Inflamm.* **2020** (3872367). https://doi.org/10.1155/2020/3872367 (2020).
80. Zheng, Y., Xu, L., Dong, N. & Li, F. NLRP3 inflammasome: the rising star in cardiovascular diseases. *Front. Cardiovasc. Med.* **9**, 927061. https://doi.org/10.3389/fcvm.2022.927061 (2022).
81. Kim, H. J., Kim, H., Lee, J. H. & Hwangbo, C. Toll-like receptor 4 (TLR4): new insight immune and aging. *Immun. Ageing*. **20**, 67. https://doi.org/10.1186/s12979-023-00383-3 (2023).
82. Guex, N. & Peitsch, M. C. SWISS-MODEL and the Swiss-PdbViewer: an environment for comparative protein modeling. *Electrophoresis* **18**, 2714–2723. https://doi.org/10.1002/elps.1150181505 (1997).
83. Tian, W., Chen, C., Lei, X., Zhao, J. & Liang, J. CASTp 3.0: computed atlas of surface topography of proteins. *Nucleic Acids Res.* **46**, 363–367. https://doi.org/10.1093/nar/gky473 (2018).

84. Lan, J. et al. Structure of the SARS-CoV-2 Spike receptor-binding domain bound to the ACE2 receptor. *Nature* **581**, 215–220. https://doi.org/10.1038/s41586-020-2180-5 (2020).
85. Thompson, D., Pepys, M. B. & Wood, S. P. The physiological structure of human C-reactive protein and its complex with phosphocholine. *Structure* **7**, 169–177. https://doi.org/10.1016/S0969-2126(99)80023-9 (1999).
86. Rowsell, S. et al. Crystal structure of human MMP9 in complex with a reverse hydroxamate inhibitor. *J. Mol. Biol.* **319**, 173–181. https://doi.org/10.1016/S0022-2836(02)00262-0 (2002).
87. Sharif, H. et al. Structural mechanism for NEK7-licensed activation of NLRP3 inflammasome. *Nature* **570**, 338–343. https://doi.org/10.1038/s41586-019-1295-z (2019).
88. Park, B. S. et al. The structural basis of lipopolysaccharide recognition by the TLR4–MD-2 complex. *Nature* **458**, 1191–1195. https://doi.org/10.1038/nature07830 (2009).
89. Huang, L. et al. Novel peptide inhibitors of angiotensin-converting enzyme 2. *J. Biol. Chem.* **278**, 15532–15540. https://doi.org/10.1074/jbc.M212934200 (2003).
90. Wang, G., Li, Y. & Li, X. Correlation of Three-dimensional structures with the antibacterial activity of a group of peptides designed based on a nontoxic bacterial membrane Anchor *. *J. Biol. Chem.* **280**, 5803–5811. https://doi.org/10.1074/jbc.M410116200 (2005).
91. Hoover, D. M.et al. The Structure of Human β-Defensin-2 Shows Evidence of Higher Order Oligomerization*. *Journal of Biological Chemistry* 275, 32911–32918, doi:10.1074/jbc.M006098200 (2000).
92. Zangger, K., Gößler, R., Khatai, L., Lohner, K. & Jilek, A. Structures of the glycine-rich diastereomeric peptides Bombinin H2 and H4. *Toxicon* **52**, 246–254. https://doi.org/10.1016/j.toxicon.2008.05.011 (2008).
93. Wang, G. Structures of human host defense Cathelicidin LL-37 and its smallest antimicrobial peptide KR-12 in lipid Micelles *. *J. Biol. Chem.* **283**, 32637–32643. https://doi.org/10.1074/jbc.M805533200 (2008).
94. Oh, D. et al. NMR structural characterization of cecropin A(1–8) - magainin 2(1–12) and cecropin A (1–8) - melittin (1–12) hybrid peptides. *J. Pept. Res.* **53**, 578–589. https://doi.org/10.1034/j.1399-3011.1999.00067.x (1999).
95. de Viana, T. et al. Release of Immunomodulatory peptides at bacterial membrane interfaces as a novel strategy to fight microorganisms. *J. Biol. Chem.* **299** https://doi.org/10.1016/j.jbc.2023.103056 (2023).
96. Nguyen, V. S., Tan, K. W., Ramesh, K., Chew, F. T. & Mok, Y. K. Structural basis for the bacterial membrane insertion of Dermcidin peptide, DCD-1L. *Sci. Rep.* **7**, 13923. https://doi.org/10.1038/s41598-017-13600-z (2017).
97. Loffredo, M. R. et al. Membrane perturbing activities and structural properties of the frog-skin derived peptide Esculentin-1a(1–21)NH2 and its diastereomer Esc(1–21)-1c: correlation with their antipseudomonal and cytotoxic activity. *Biochim. Et Biophys. Acta (BBA) - Biomembr.* **1859**, 2327–2339. https://doi.org/10.1016/j.bbamem.2017.09.009 (2017).
98. Runge, S., Thøgersen, H., Madsen, K., Lau, J. & Rudolph, R. Crystal structure of the Ligand-bound Glucagon-like Peptide-1 receptor extracellular Domain *. *J. Biol. Chem.* **283**, 11340–11347. https://doi.org/10.1074/jbc.M708740200 (2008).
99. Jordan, J. B. et al. Hepcidin revisited, disulfide connectivity, dynamics, and structure < sup >. *J. Biol. Chem.* **284**, 24155–24167. https://doi.org/10.1074/jbc.M109.017764 (2009).
100. Mariano, G. H. et al. Characterization of novel human intragenic antimicrobial peptides, incorporation and release studies from ureasil-polyether hybrid matrix. *Mater. Sci. Engineering: C.* **119**, 111581. https://doi.org/10.1016/j.msec.2020.111581 (2021).
101. Friedrich, C. L., Rozek, A., Patrzykat, A. & Hancock, R. E. W. Structure and mechanism of action of an Indolicidin peptide derivative with improved activity against Gram-positive Bacteria *. *J. Biol. Chem.* **276**, 24015–24022. https://doi.org/10.1074/jbc.M009691200 (2001).
102. Hwang, P. M., Zhou, N., Shan, X., Arrowsmith, C. H. & Vogel, H. J. Three-Dimensional solution structure of lactoferricin B, an antimicrobial peptide derived from bovine lactoferrin. *Biochemistry* **37**, 4288–4298. https://doi.org/10.1021/bi972323m (1998).
103. Pillong, M. et al. Rational design of Membrane-Pore-Forming peptides. *Small* **13**, 1701316. https://doi.org/10.1002/smll.201701316 (2017).
104. Gesell, J., Zasloff, M. & Opella, S. J. Two-dimensional 1H NMR experiments show that the 23-residue Magainin antibiotic peptide is an α-helix in Dodecylphosphocholine micelles, sodium dodecylsulfate micelles, and trifluoroethanol/water solution. *J. Biomol. NMR.* **9**, 127–135. https://doi.org/10.1023/A:1018698002314 (1997).
105. Terwilliger, T. C., Weissman, L. & Eisenberg, D. The structure of Melittin in the form I crystals and its implication for Melittin's lytic and surface activities. *Biophys. J.* **37**, 353–361. https://doi.org/10.1016/s0006-3495(82)84683-3 (1982).
106. Mathavan, I. et al. Structural basis for hijacking siderophore receptors by antimicrobial Lasso peptides. *Nat. Chem. Biol.* **10**, 340–342. https://doi.org/10.1038/nchembio.1499 (2014).
107. Hsu, S. T. D. et al. The nisin–lipid II complex reveals a pyrophosphate cage that provides a blueprint for novel antibiotics. *Nat. Struct. Mol. Biol.* **11**, 963–967. https://doi.org/10.1038/nsmb830 (2004).
108. Bhunia, A. et al. NMR structure of pardaxin, a Pore-forming antimicrobial peptide, in lipopolysaccharide micelles: MECHANISM OF OUTER MEMBRANE PERMEABILIZATION 2 < sup >. *J. Biol. Chem.* **285**, 3883–3895. https://doi.org/10.1074/jbc.M109.065672 (2010).
109. Comert, F. et al. The host-defense peptide piscidin P1 reorganizes lipid domains in membranes and decreases activation energies in mechanosensitive ion channels. *J. Biol. Chem.* **294**, 18557–18570. https://doi.org/10.1074/jbc.RA119.010232 (2019).
110. Amos, S. T. et al. Antimicrobial peptide potency is facilitated by greater conformational flexibility when binding to Gram-negative bacterial inner membranes. *Sci. Rep.* **6**, 37639. https://doi.org/10.1038/srep37639 (2016).
111. Powers, J. P. S., Rozek, A. & Hancock, R. E. W. Structure–activity relationships for the β-hairpin cationic antimicrobial peptide polyphemusin I. *Biochimica et Biophysica Acta (BBA) - Proteins and Proteomics* 1698, 239–250, (2004). https://doi.org/10.1016/j.bbapap.2003.12.009
112. Fahrner, R. L. et al. Solution structure of protegrin-1, a broad-spectrum antimicrobial peptide from Porcine leukocytes. *Chem. Biol.* **3**, 543–550. https://doi.org/10.1016/s1074-5521(96)90145-3 (1996).
113. Petit, V. W. et al. A hemocyanin-derived antimicrobial peptide from the Penaeid shrimp adopts an alpha-helical structure that specifically permeabilizes fungal membranes. *Biochim. Et Biophys. Acta (BBA) - Gen. Subj.* **1860**, 557–568. https://doi.org/10.1016/j.bbagen.2015.12.010 (2016).
114. Kawulka, K. E. et al. Structure of subtilosin A, a Cyclic antimicrobial peptide from Bacillus subtilis with unusual sulfur to α-Carbon Cross-Links: formation and reduction of α-Thio-α-Amino acid derivatives. *Biochemistry* **43**, 3385–3395. https://doi.org/10.1021/bi0359527 (2004).
115. Kushibiki, T. et al. Interaction between Tachyplesin I, an antimicrobial peptide derived from horseshoe crab, and lipopolysaccharide. *Biochim. Et Biophys. Acta (BBA) - Proteins Proteom.* **1844**, 527–534. https://doi.org/10.1016/j.bbapap.2013.12.017 (2014).
116. Fujitani, N. et al. Structure of the antimicrobial peptide Tachystatin A *. *J. Biol. Chem.* **277**, 23651–23657. https://doi.org/10.1074/jbc.M111120200 (2002).
117. Manzo, G. et al. Temporin L and aurein 2.5 have identical conformations but subtly distinct membrane and antibacterial activities. *Sci. Rep.* **9**, 10934. https://doi.org/10.1038/s41598-019-47327-w (2019).
118. Mandard, N. et al. Solution structure of Thanatin, a potent bactericidal and fungicidal insect peptide, determined from proton two-dimensional nuclear magnetic resonance data. *Eur. J. Biochem.* **256**, 404–410. https://doi.org/10.1046/j.1432-1327.1998.2560404.x (1998).
119. Fiebig, D. et al. Destructive twisting of neutral metalloproteases: the catalysis mechanism of the dispase autolysis-inducing protein from Streptomyces mobaraensis DSM 40487. *FEBS J.* **285**, 4246–4264. https://doi.org/10.1111/febs.14647 (2018).

120. Mehdi, S. F. et al. Glucagon-like peptide-1: a multi-faceted anti-inflammatory agent. *Front. Immunol.* **14**, 1148209. https://doi.org/10.3389/fimmu.2023.1148209 (2023).
121. Sortino, O. et al. The effects of Recombinant human lactoferrin on immune activation and the intestinal Microbiome among persons living with human immunodeficiency virus and receiving antiretroviral therapy. *J. Infect. Dis.* **219**, 1963–1968. https://doi.org/10.1093/infdis/jiz042 (2019).
122. Agier, J., Efenberger, M. & Brzezińska-Błaszczyk, E. Cathelicidin impact on inflammatory cells. *Cent. Eur. J. Immunol.* **40**, 225–235. https://doi.org/10.5114/ceji.2015.51359 (2015).
123. Dominguez, C., Boelens, R. & Bonvin, A. M. J. J. HADDOCK: A Protein – Protein Docking approach based on biochemical or biophysical information. *J. Am. Chem. Soc.* **125**, 1731–1737. https://doi.org/10.1021/ja026939x (2003).
124. Jumper, J. et al. Highly accurate protein structure prediction with alphafold. *Nature* **596**, 583–589. https://doi.org/10.1038/s41586-021-03819-2 (2021).
125. Vangone, A. & Bonvin, A. P. R. O. D. I. G. Y. A Contact-based predictor of binding affinity in Protein-protein complexes. *BIO-PROTOCOL* **7** https://doi.org/10.21769/BioProtoc.2124 (2017).
126. Grassmann, G. et al. Computational approaches to predict Protein–Protein interactions in crowded cellular environments. *Chem. Rev.* **124**, 3932–3977. https://doi.org/10.1021/acs.chemrev.3c00550 (2024).
127. Pronk, S. et al. GROMACS 4.5: a high-throughput and highly parallel open source molecular simulation toolkit. *Bioinformatics* **29**, 845–854. https://doi.org/10.1093/bioinformatics/btt055 (2013).
128. Saini, R. S. et al. In silico assessment of biocompatibility and toxicity: molecular docking and dynamics simulation of PMMA-based dental materials for interim prosthetic restorations. *Journal of Materials Science: Materials in Medicine* 35, 28, (2024). https://doi.org/10.1007/s10856-024-06799-7
129. Yuet, P. & Blankschtein, D. Molecular dynamics simulation study of water surfaces: comparison of flexible water models. *J. Phys. Chem.* **114**, 13786–13795. https://doi.org/10.1021/jp1067022 (2010).
130. Saini, R. S. et al. Dental biomaterials redefined: molecular Docking and dynamics-driven dental resin composite optimization. *BMC Oral Health*. **24**, 557. https://doi.org/10.1186/s12903-024-04343-1 (2024).
131. The PyMOL Molecular Graphics System v. 2.4. (2020).
132. Pettersen, E. F. et al. UCSF Chimera–a visualization system for exploratory research and analysis. *J. Comput. Chem.* **25**, 1605–1612. https://doi.org/10.1002/jcc.20084 (2004).
133. Tian, S. et al. Assessing an ensemble docking-based virtual screening strategy for kinase targets by considering protein flexibility. *J. Chem. Inf. Model.* **54**, 2664–2679. https://doi.org/10.1021/ci500414b (2014).
134. Yuan, Z. et al. Binding free energy calculation based on the fragment molecular orbital method and its application in designing novel SHP-2 allosteric inhibitors. *Int. J. Mol. Sci.* **25**, 1–24 (2024).
135. Rifai, E. A., Ferrario, V., Pleiss, J. & Geerke, D. P. Combined linear interaction energy and alchemical solvation Free-Energy approach for Protein-Binding affinity computation. *J. Chem. Theory Comput.* **16**, 1300–1310. https://doi.org/10.1021/acs.jctc.9b00890 (2020).
136. Valdés-Tresanco, M. S., Valdés-Tresanco, M. E., Valiente, P. A., Moreno, E. & gmx_MMPBSA A new tool to perform End-State free energy calculations with GROMACS. *J. Chem. Theory Comput.* **17**, 6281–6291. https://doi.org/10.1021/acs.jctc.1c00645 (2021).
137. Miller, B. R. 3 et al. MMPBSA.py: an efficient program for End-State free energy calculations. *J. Chem. Theory Comput.* **8**, 3314–3321. https://doi.org/10.1021/ct300418h (2012).
138. Panday, S. K. & Alexov, E. Protein-Protein binding free energy predictions with the MM/PBSA approach complemented with the Gaussian-Based method for entropy Estimation. *ACS Omega*. **7**, 11057–11067. https://doi.org/10.1021/acsomega.1c07037 (2022).
139. Timmons, P. B. & Hewage, C. M. HAPPENN is a novel tool for hemolytic activity prediction for therapeutic peptides which employs neural networks. *Sci. Rep.* **10**, 10869. https://doi.org/10.1038/s41598-020-67701-3 (2020).
140. Gasteiger, E. et al. in *In the Proteomics Protocols Handbook*. 571–607 (eds Walker, J. M.) (Humana, 2005).

Author contributions

D.D. and N.A. contributed to the conception, design and supervision of the work and revision of the manuscript. D.D. contributed to the acquisition and analysis of the computational data/results. D.D. and N.A. wrote the manuscript. All authors have read and approved the final manuscript.

Funding

This work was supported and funded by the Deanship of Scientific Research at Imam Mohammad Ibn Saud Islamic University (IMSIU) (grant number IMSIU-DDRSP2501).

Declarations

Competing interests

The authors declare no competing interests.

Additional information

Supplementary Information The online version contains supplementary material available at https://doi.org/10.1038/s41598-025-93683-1.

Correspondence and requests for materials should be addressed to N.A.

Reprints and permissions information is available at www.nature.com/reprints.

Publisher's note Springer Nature remains neutral with regard to jurisdictional claims in published maps and institutional affiliations.